UCRL 8848

UNIVERSITY OF CALIFORNIA
Ernest O. Lawrence
Radiation Laboratory

BIO-ORGANIC CHEMISTRY QUARTERLY REPORT
March, April, May 1959

TWO-WEEK LOAN COPY

This is a Library Circulating Copy which may be borrowed for two weeks. For a personal retention copy, call Tech. Info. Division, Ext. 5545

DISCLAIMER

This document was prepared as an account of work sponsored by the United States Government. While this document is believed to contain correct information, neither the United States Government nor any agency thereof, nor the Regents of the University of California, nor any of their employees, makes any warranty, express or implied, or assumes any legal responsibility for the accuracy, completeness, or usefulness of any information, apparatus, product, or process disclosed, or represents that its use would not infringe privately owned rights. Reference herein to any specific commercial product, process, or service by its trade name, trademark, manufacturer, or otherwise, does not necessarily constitute or imply its endorsement, recommendation, or favoring by the United States Government or any agency thereof, or the Regents of the University of California. The views and opinions of authors expressed herein do not necessarily state or reflect those of the United States Government or any agency thereof or the Regents of the University of California.

UCRL-8848
Chemistry - General
TID-4500 (15th Ed.)

UNIVERSITY OF CALIFORNIA
Lawrence Radiation Laboratory
Berkeley, California

Contract No. W-7405-eng-48

BIO-ORGANIC CHEMISTRY QUARTERLY REPORT

March, April, May 1959

June 30, 1959

Printed for the U. S. Atomic Energy Commission

Printed in USA. Price $2.25. Available from the
Office of Technical Services
U. S. Department of Commerce
Washington 25, D. C.

BIO-ORGANIC CHEMISTRY QUARTERLY REPORT

March, April, May 1959

Contents

Electrical Properties of Metal-Free Phthalocyanine: Kinetics and Mechanism of Conductivity
Gordon Tollin and David R. Kearns 3

Quantum Yield of Photo-Induced Unpaired Electrons in Spinach Chloroplasts
Lou Ann Carter and Power B. Sogo 27

The Hill Reaction and $C^{14}O_2$ Fixation in Intact, Washed and Fragmented Chloroplasts
R. B. Park, K. P. Louwrier and N. G. Pon . 28

Biodynamics of Carbon Reduction During Photosynthesis
J. A. Bassham and M. Kirk 32

Preliminary Incubation Studies of Carboxydismutase
Ning G. Pon 46

Biosynthesis of Morphine Alkaloids
Frank R. Stermitz and Henry Rapoport . . . 52

Adenine Metabolism in Mice Maintained on Deuterium Oxide
Edward L. Bennett and Nancy Dye 55

Protein Content of Rat Brain -- Strain and Area Differences
E. L. Bennett, Ann Ohlander and Hiromi Morimoto 58

Effect of Crystal Size on the Radiation Sensitivity of Choline Chloride
Richard M. Lemmon and Bernice Soltysik . . 66

The Chemistry of N-Carboxy-L-Glutamic Acid Anhydride: A Preliminary Report
Yoshiro Ogata 68

*Preceding Quarterly Reports: UCRL-8698, UCRL-8575

BIO-ORGANIC CHEMISTRY QUARTERLY REPORT

March, April, May 1959

M. Calvin, Director

Edited by J. A. Bassham

Lawrence Radiation Laboratory and Department of Chemistry
University of California, Berkeley, California

June 30, 1959

ELECTRICAL PROPERTIES OF METAL-FREE PHTALOCYANINE: KINETICS AND MECHANISM OF CONDUCTIVITY

Gordon Tollin and David R. Kearns

A. Introduction

Previous work from this laboratory[1] has suggested that the mechanism of quantum conversion in photosynthesis involves processes which are characteristic of ordered arrays of pigment molecules. For this reason, it has seemed important to investigate in detail the electronic properties of such systems. Furthermore, investigations of this nature are of great interest in their own right. With this in mind, techniques have been developed which permit the study of the kinetics of photoconductivity in solid organic dye materials.

B. Materials and Methods

The material used in the experiments was prepared from crude metal-free phthalocyanine (DuPont) by vacuum sublimation in a muffle furnace. This yielded crystalline material in the form of needles 0.1 to 1 cm. in length. The cell used for most of the conductivity measurements is diagrammed in Fig. 1. Additional measurements were also carried out using a sandwich-type cell. The samples were applied to the electrodes by another vacuum sublimation of the crystalline material. A variety of ambient atmospheres (air, O_2, N_2, natural gas) were used in the sublimations, but the results appeared to be independent of the gas used. Subsequent to the sublimation of the sample, the entire cell was coated with a clear acrylic resin. This coating served merely a protective function and produced no changes in any of the measured properties of the phthalocyanine. For the conductivity measurements, the sample cell was mounted on one end of a copper rod, the temperature of which could be varied. For most of the measurements, field strengths of the order of 10^4 volts/cm were used. X-ray diffraction indicated that the sublimed films of phthalocyanine were essentially amorphous. However, the films could be made microcrystalline by annealing the entire cell at 270° for several days under reduced natural gas pressure. The crystals formed

[1] Tollin, Sogo, and Calvin, Ann. N. Y. Acad. Sci. 74, 310 (1958).

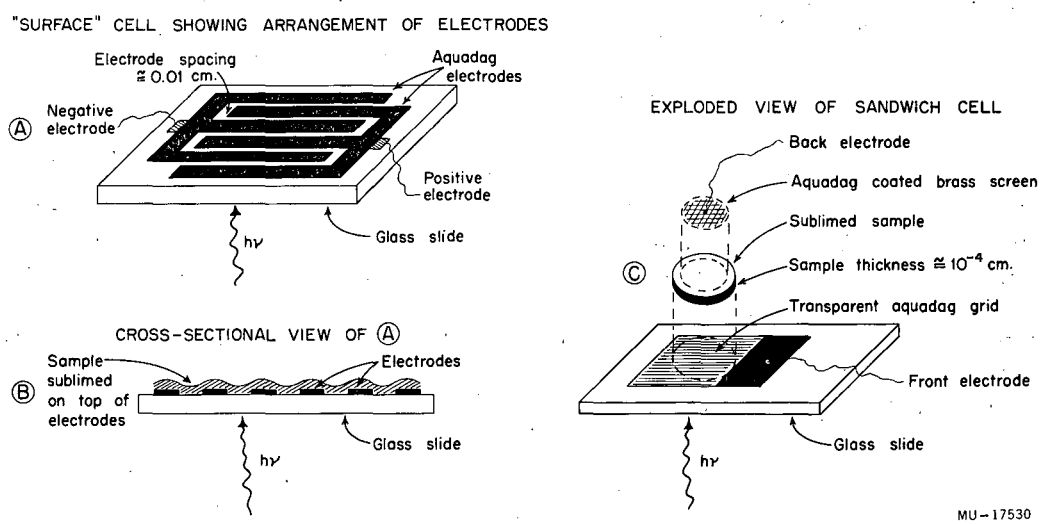

Fig. 1. Diagram of sample cells.

in this manner were about 1 micron in diameter and 10 μ long.

Figure 2 shows a block diagram of the apparatus used in these studies. For kinetic studies, the samples were illuminated by a General Electric FT-230 flashtube operated at 1500 volts with a load capacitance of 2 microfarads. This produced a light pulse with a 1-microsecond rise time which decayed to about 10% of its peak intensity in about 5 μsec. A standard triggering system was used.

Photocurrent generated in the sample by the light pulse was passed through a known resistance with values ranging from 1000 to 100,000 ohms, depending upon the experiment. The voltage developed across this resistance was fed through a cathode follower and d.c. amplifier (gain=2000) into the various recording devices. In this manner, it was possible to measure the decay curve of the photocurrent from about 10 μsec after flashing to about 100 sec. The photosignal itself was used to trigger the oscilloscope sweep and thus it was also possible to observe the rise time of the photocurrent.

For the measurement of action spectra and steady-state photoconductivity, a Hanovia 800-watt xenon arc lamp and a Bausch and Lomb 500-mm grating monochromator were used in place of the flashtube.

C. Results and Discussion

1. Kinetics of Photocurrent Decay

Typical photocurrent decay-curve data are shown in Fig. 3. These were obtained with unannealed metal-free phthalocyanine in the "surface" cell shown in Fig. 1. Unless otherwise stated, all the following results apply to samples of this type. It is apparent that the rise time of the photocurrent is limited by the rise time of the flash (~1 μsec).

In Fig. 4, a plot of log photocurrent $(\frac{i}{e})$ vs log time (t) is shown for data obtained at 23°C and at -35°C. From these curves it is apparent that the current decay from several hundred microseconds to several seconds obeys the relation

$$I = \frac{i}{e} = c\,t^{y}, \qquad (1)$$

where e is electronic charge, and y is - 1/2 at 23°C and -0.43 at -35°C. This was the general result for all the samples studied under all conditions, with y varying between -0.6 and -0.4.

The curves in Fig. 4 also show a break at longer times (greater than 1 sec at 23°C and greater than 15 sec at -35°C) with y approaching -1. If one replots the long-time data, it is possible to show that the curves follow a bimolecular law,

$$1/I = K\,t + \text{constant}. \qquad (2)$$

Such plots are shown in Fig. 5 for both 23°C and -35°C. Thus, at low

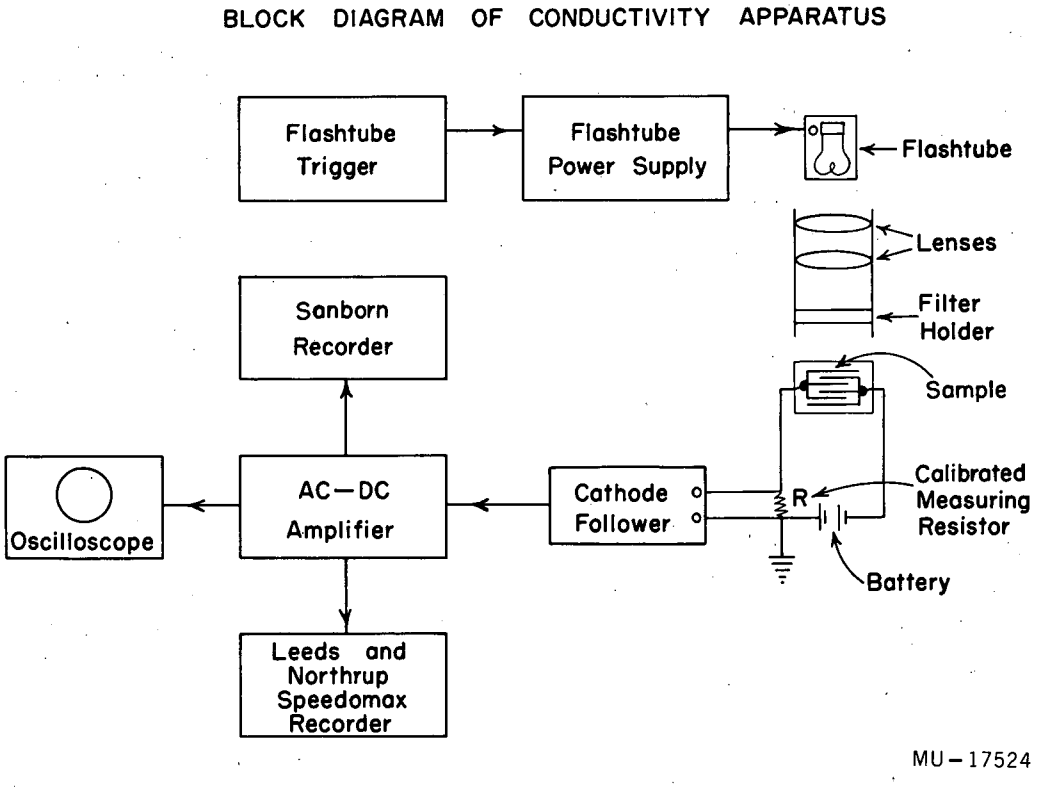

Fig. 2. Block diagram of conductivity apparatus.

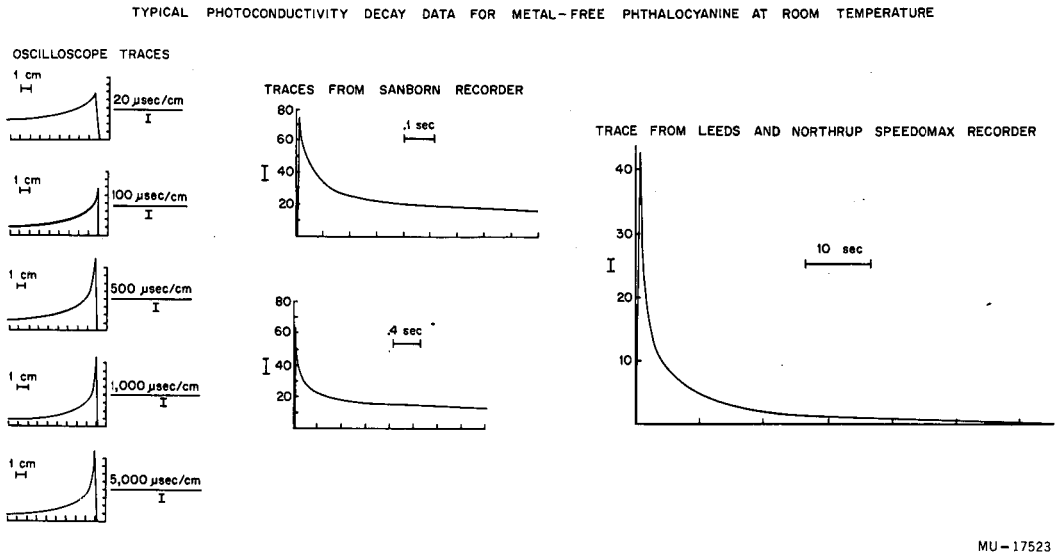

Fig. 3. Typical photoconductivity decay data for metal-free phthalocyanine at room temperature.

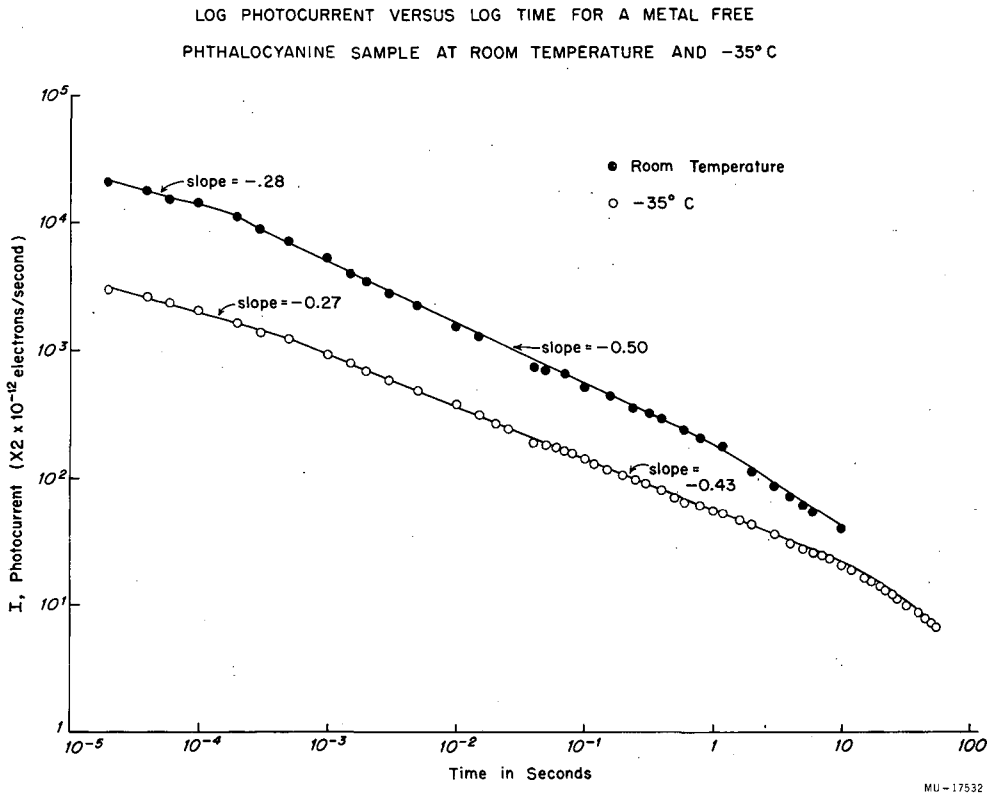

Fig. 4. Log photocurrent vs log time for a metal-free phthalocyanine sample at room temperature and at -35°C.

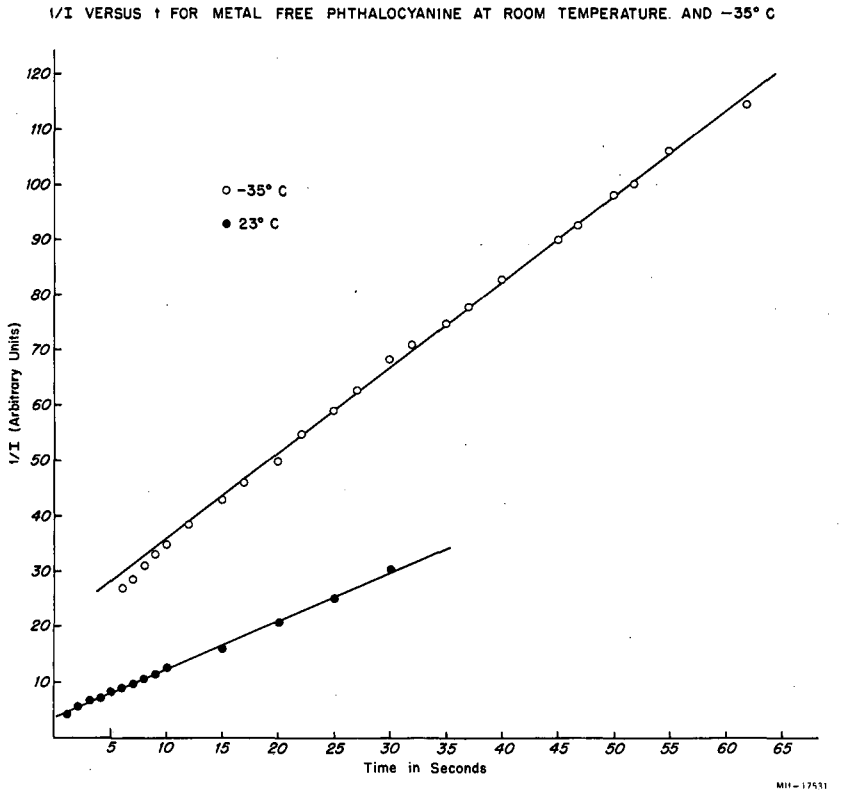

Fig. 5. 1/I vs t for metal-free phthalocyanine at room temperature and at -35°C.

carrier concentrations the decay is strictly bimolecular, and at higher carrier concentrations the decay is slower than bimolecular.

At the shortest times (10 to 100 μsec), the current decays even more slowly than at the longer times (>100 μsec).

The decay law at low current is precisely what one would expect for a process involving the recombination of oppositely charged carriers. The slower decay at the higher currents may be accounted for simply by assuming a concentration-dependent charge-carrier mobility, analagous to what is observed for ion mobilities in solutions of high ionic strength.[2]

If one makes the above assumptions, it is possible to obtain an equation which adequately expresses the time dependence of the photocurrent at all except the very earliest times (<100 μsec). An empirical relation between current I and carrier concentration n, which will lead to a satisfactory description of the experimental results, is

$$I = \frac{\mu_0}{(n + c)^{1-1/x}} \cdot nAE, \tag{3}$$

where n = total carrier concentration = $n_+ + n_-$,

E = field strength,

A = cross-sectional area of conducting material,

$\bar{\mu} = \dfrac{\mu_0}{(n + c)^{1-1/x}}$ = apparent average carrier mobility at a particular value of n,

and c and x are constants for a given sample and temperature, c representing a critical concentration of carriers below which the mobility is concentration-independent.

Assuming a bimolecular rate law,

$$dn/dt = -K n^2, \tag{4}$$

where K = rate constant (units of cm^3/sec carrier), one can derive the following equations.
At $n \ll c$:

$$I = \frac{\mu_0}{(c)^{1-1/x}} \cdot nAE. \tag{5}$$

[2] W. J. Moore, Physical Chemistry (Prentice-Hall, New York, 1950), p. 451.

Substituting Eq. (5) in (4) yields

$$\frac{dI}{dt} = - \frac{Kc^{1-1/x}}{\mu_0 AE} \cdot I^2, \tag{6}$$

or, upon integration,

$$1/I = \frac{Kc^{1-1/x}}{\mu_0 AE} t + \text{constant}. \tag{7}$$

For $n \gg c$:

$$I = \mu_0 n^{1/x} AE, \tag{8}$$

and upon substitution in Eq. (4) and integration, one obtains

$$I = \frac{\mu_0 AE}{K^{1/x}} t^{-1/x} + \text{constant}. \tag{9}$$

Thus, at low carrier concentrations, I should decay according to Eq. (7) and at high carrier concentrations according to Eq. (9), in agreement with experiment.

It is also possible to write equations for the steady-state photoconductivity. At the steady state, Eq. (4) becomes

$$\frac{dn}{dt} = 0 = -Kn^2 + L, \tag{10}$$

where L = rate of photoproduction of charge carriers; L is proportional to light intensity, the proportionality factor involving the quantum yield.

At high light intensity, Eq. (8) applies, and one obtains, upon substitution in (10),

$$I_{\substack{\text{steady state} \\ \text{(high light)}}} = \frac{\mu_0 AE}{K^{1/2x}} \cdot L^{1/2x}. \tag{11}$$

At low light intensities, Eq. (5) applies, and upon substitution into (10), one obtains

$$I_{\substack{\text{steady state} \\ \text{(low light)}}} = \frac{\mu_0 AE}{c^{1-1/x} K^{1/2}} L^{1/2} \tag{12}$$

From the room-temperature curve of Fig. 4, it is apparent that x = 2 under these conditions. Thus, for this sample, the steady-state photocurrent should vary as the fourth root of the light intensity at very high light intensities, if the mechanism proposed above is correct. That

this is approximately the case is demonstrated by Fig. 6. These data were obtained by focusing the unfiltered light from the 800-watt xenon arc lamp through a water bath onto the sample. At low light intensities, Eq. (12) predicts that the steady-state photocurrent should vary as the square root of the light intensity. That this is so is also shown in Fig. 6.

It has been observed[3] in cells in which only surface conductivity is measured that at very low light intensities the steady-state photocurrent is roughly linear with the light intensity. Even at the lowest light intensities obtainable, this behavior is not observed in the samples reported here. This is similar to the results found with sandwich-type cells when bulk properties are being measured.[3] The similarity suggests that the measurements reported here related predominantly to bulk properties. This is plausible in view of the geometry of the "surface" cells used here (see Fig. 1).

The fact that photocurrents may be observed for several minutes after flash illumination suggests that carrier recombination may be diffusion-limited. The mathematics of diffusion-limited reactions have been treated by Waite.[4] For a bimolecular diffusion-limited process, Waite derives the following expression for the rate law at low reactant concentrations:

$$dn/dt = 4 \pi r_0 D n^2 = - K n_2 \tag{13}$$

where r_0 = distance of separation of reactants within which reaction is rapid, but beyond of which there is essentially no interaction,

D = diffusivity (units of cm^2/sec-carrier),

K = bimolecular rate constant, as previously defined in Eq. (4),

n = concentration of holes = concentration of electrons.

Therefore

$$K = 4 \pi r_0 D. \tag{14}$$

From the Einstein equation,[5]

$$D = \frac{\mu kT}{e}, \tag{15}$$

where--in this case, we have

$$\mu = \frac{\mu_0}{c^{1-1/x}} \quad -- \tag{16}$$

[3] D. M. J. Compton, W. G. Schneider and T. C. Waddington, J. Chem. Phys. 27, 160 (1957).

[4] T. R. Waite, Phys. Rev. 107, 463 (1957).

[5] N. F. Mott and R. W. Gurney, "Electronic Processes in Ionic Crystals" (Clarendon Press Oxford, 1950), p. 63.

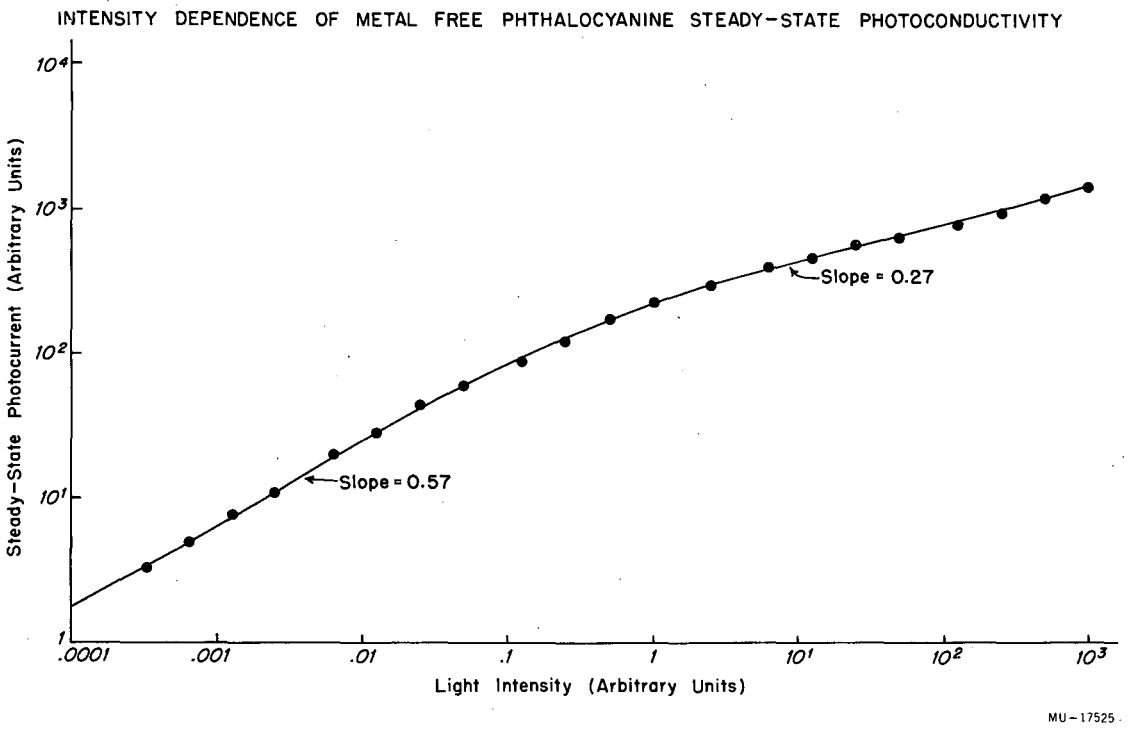

Fig. 6. Intensity dependence of metal-free phthalocyanin steady-state photoconductivity.

the following equation is obtained:

$$K = 4 \pi r_0 \frac{\mu_0}{c^{1-1/x}} \cdot \frac{kT}{e} . \tag{17}$$

From Eq. (7), the slope of a plot of 1/I vs t at low I is equal to

$$\frac{Kc^{1-1/x}}{\mu_0 AE} = B. \tag{18}$$

Substitution of Eq. (17) into (18) gives

$$\frac{4 \pi r_0}{AE} \cdot \frac{kT}{e} = B, \tag{19}$$

or rearranging,

$$r_0 = \frac{BAE}{4 \pi} \cdot \frac{e}{kT} . \tag{20}$$

This equation permits the calculation of r_0 from experimental data. For metal-free phthalocyanine at room temperature, r_0 is approximately 25 A (about one molecular diameter) and increases to several hundred angstroms at -35°C. At temperatures up to 50°C, r_0 remained at about the room-temperature value, within experimental error.

The fact that one can obtain reasonable values for r_0 suggests that the assumption that recombination is diffusion-limited is moderately accurate. The observed increase in r_0 at low temperatures may then be attributed to a decrease in thermal scattering.

2. Results with Sandwich Cells and Annealed Samples

Room-temperature photoconductivity decay curves were also measured for sandwich-type cells of metal-free phthalocyanine. These gave essentially the same kinetics as did the "surface" cells. In general, the sandwich cells were more difficult to prepare and their signal-to-noise ratio was only about 1/100 that of the "surface" cells.

A common method used to indicate the sign of the majority charge carrier in a sandwich cell is to measure the magnitude of the photocurrent as a function of the polarity of the illuminated electrode. When this was done for a sandwich cell of metal-free phthalocyanine, it was found that higher currents (about double) were obtained when the illuminated electrode was positive than when it was negative. This indicates that holes are the more mobile carriers, in agreement with investigations of other organic compounds.[6]

[6] P. E. Fielding and F. Gutman, J. Chem. Phys. 26, 411 (1957).

Microcrystalline (annealed) "surface" cells exhibit the same photocurrent kinetic behavior as do the unannealed samples. However, the annealed samples exhibit a lower concentration dependence of carrier mobility. It is to be expected that more ordered samples would contain fewer scattering centers and therefore possess higher carrier mobilities. This is consistent with obtaining higher photocurrents with annealed samples than with unannealed samples, under identical conditions. Thus, it would appear that for lower carrier mobilities the carrier-mobility concentration dependences are higher. It is planned to investigate the microcrystalline samples in greater detail in the future.

3. Temperature Dependence of Current Decay

A change in temperature over the range from 60°C to -35°C does not affect the kinetics of the major portion of the decay curve (20μsec seconds to 100 sec), within experimental error. In particular, the photocurrent decay remains bimolecular at low currents, indicating that there are no trapping centers with depths greater than about 0.05 ev.

A decrease in temperature was found to cause a slight decrease in the $1/x$ value. For example, $1/x = 0.50$ at 23°C and $1/z = 0.43$ at -35°C, as shown in Fig. 4. Inasmuch as one would expect a decrease in mobility at lower temperatures, these results again indicate that there is an inverse relationship between mobility and concentration dependence of mobility. This is further demonstrated by the fact that the concentration-dependent portion of the decay curve extends to longer times at the lower temperature (see Fig. 4).

4. Temperature Dependence of Steady-State Photocurrent and Dark Current

The steady-state photocurrent as a function of temperature obeyed the equation[6a]

$$I_{\text{steady-state}} = c\,e^{-\Delta E/kT}, \tag{21}$$

where $\Delta E \cong 0.2$ ev, in agreement with other reported values.

The temperature dependence of the dark current was more difficult to measure, but was found to obey the relation[6b]

$$I_{\text{dark}} = c\,e^{-\Delta E/2kT}, \tag{22}$$

where $\Delta E \cong 1\text{-}2$ ev, again in agreement with reported values.

[6a] J. Kommandeur, G. J. Korinek and W. G. Schneider, Can. J. Chem., 35, 998 (1957).

[6b] N. F. Mott and R. W. Gurney, ibid., pp. 156 et seq.

5. Voltage Dependence of Steady-State Photocurrent and Dark Current

Both steady-state photoconductivity and dark conductivity obeyed the relationship

$$I \propto V^{3/2}, \tag{23}$$

where V = applied voltage.

The kinetics of flash-photoconductivity decay were independent of the applied field.

6. Flash-Intensity Dependence of Photocurrent Decay

A study of the kinetics of photocurrent decay demonstrated that, for a given sample, the functional relationship between measured photocurrent, I, and carrier concentration, n, as given in Eq. (3), did not change with flash intensity, for times after flashing greater than about 200 μsec. For shorter times (<200 μsec), it was found that as the flash intensity decreased the photocurrent decayed more slowly. This is shown in Fig. 7.

7. Spectral Response of Steady-State Photoconductivity

The photoconductivity-action spectra for both thick and thin samples are shown in Fig. 8, along with the absorption spectrum of a film of metal-free phthalocyanine. It is apparent that it is light absorbed by phthalocyanine which is effective in producing photoconductivity. Furthermore, from the fact that illumination of the back side of thick samples yields an action spectrum which is the inverse of the absorption spectrum, it can be concluded that light absorbed close to the electrodes is most effective in causing photoconductivity.

8. Effect of Ambient Illumination on Photoconductivity

If a sample is illuminated with a steady light source and simultaneously subjected to flash illumination, the photocurrent due to the flash decays more rapidly than it would in the absence of the ambient light (see Fig. 9). This effect is greater with greater intensity of the ambient light. At highest ambient light intensity, the flash-photocurrent decay becomes approximately unimolecular after about 0.01 sec. This effect may be interpreted simply as a concentration effect in which the ambient-light-produced carriers are present in concentrations greater than flash-produced carriers at the longer times. This causes the flash current to decay pseudo-unimolecularly. This hypothesis is supported by the spectral response curves of the long-time decay when the wave length of the ambient light was varied. In these experiments, the sample was flashed from one side and illuminated with ambient light from the other side. It was found that the ambient light had its greatest effect on the decay curve at wave lengths that corresponded to the inverse of the phthalocyanine absorption spectrum, indicating a direct interaction between flash-produced carriers and ambient-light-produced carriers. Wave lengths in the infrared region of the spectrum had no effect on the decay, again indicating the absence of trapping.

INTENSITY DEPENDENCE OF 0-100 μSEC PHOTOCONDUCTIVITY DECAY

FOR A TYPICAL METAL FREE PHTHALOCYANINE SAMPLE

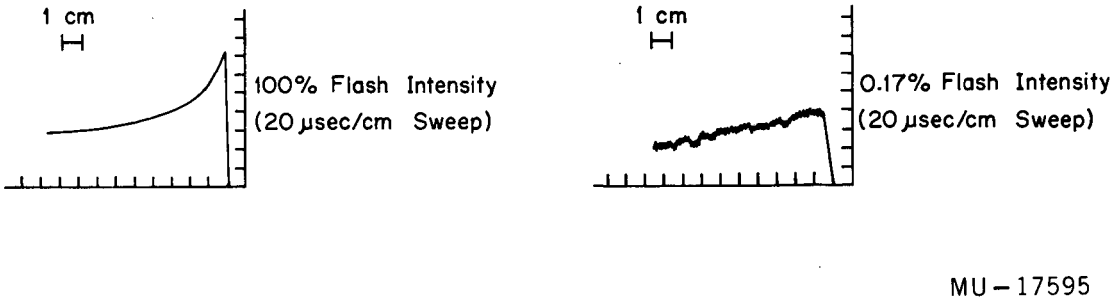

MU-17595

Fig. 7. Intensity dependence of 0 to 100 μsec photoconductivity decay for a typical metal-free phthalocyanine sample.

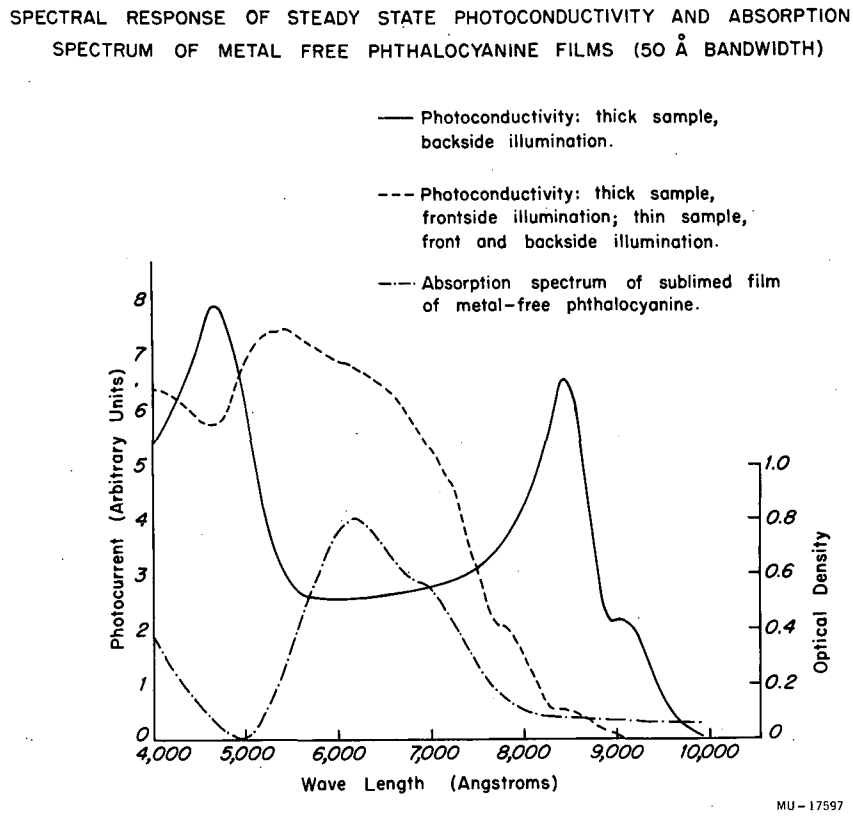

Fig. 8. Spectral response of steady-state photoconductivity and absorption spectrum of metal-free phthalocyanine films (50 Å band width).

Curve A: Back illumination of a thick sample.
Curve B: Back and front illumination of a thin sample; front illumination of a thick sample.
(All action spectra were measured with constant-energy light at all wave lengths)
Curve C: Absorption spectrum of metal-free phthalocyanine sublimed on a quartz plate.

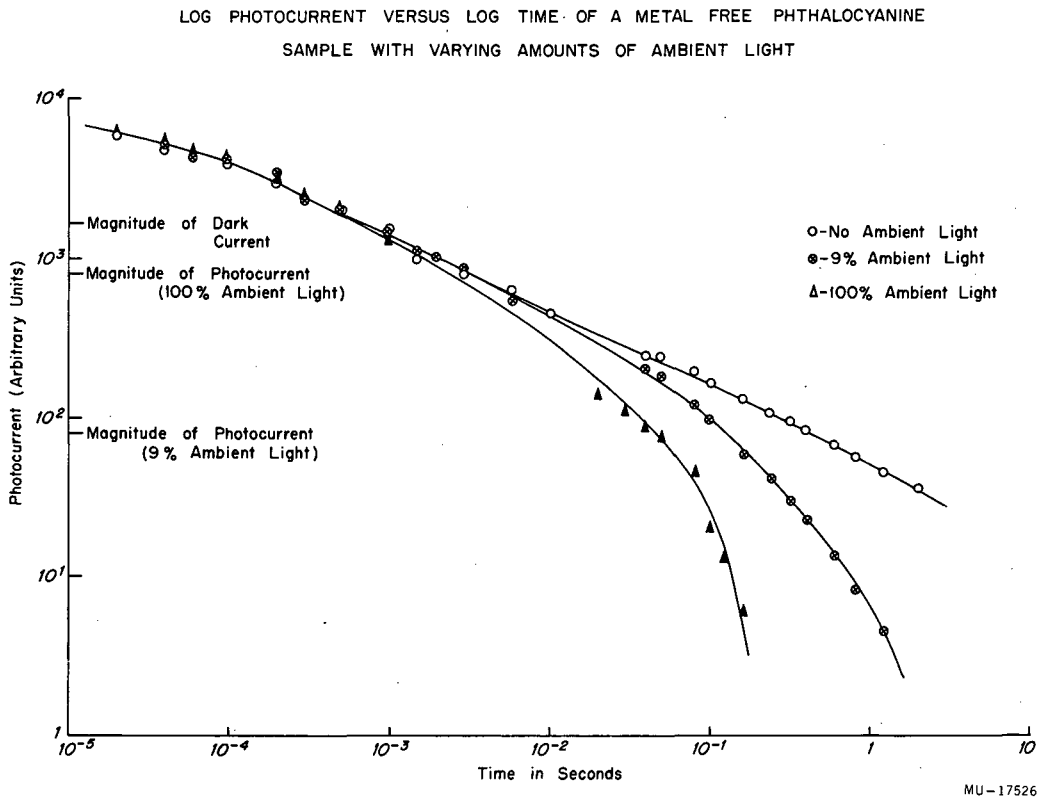

Fig. 9. Log photocurrent vs log time of a metal-face phthalocyanine sample with varying amounts of ambient

In these samples, the room-temperature dark current was approximately twice as great as the photocurrent produced by the highest-intensity ambient light. In addition, as indicated in Section 3 above, neither an increase nor a decrease in this dark current over several orders of magnitude produced any change in the kinetics of decay of the flash photocurrent. This might suggest that the measured dark current was not an intrinsic property of the phthalocyanine, but rather an artifact of the sample cell. This possibility was eliminated by the observation that the photocurrent produced by a standard light was essentially proportional to the measured dark current for a series of seven different samples. These results and the ambient-light experiments suggest that the dark current is somehow different from the photocurrent. It is not possible to explain this difference at present.

9. Electrical Properties of "Doped" Phthalocyanine

In previous experiments[7] it was observed that the electrical conductivity of organic molecular crystals was greatly enhanced and a large room-temperature electron spin resonance could be detected in the dark when these materials were treated with small quantities of oxidizing agents such as chloranil and ortho-chloranil. It was felt that an extension of this work would be of interest.

The sample cell was essentially the same as that used in the kinetic studies. The "doping" agent was applied by spraying a benzene solution onto the back of the phthalocyanine layer.

When metal-free phthalocyanine samples were treated with ortho-chloranil, the dark conductivity of the sample was increased many orders of magnitude and a large dark electron spin resonance could be observed (see Fig. 10), in agreement with previous results.[7] The increase in conductivity was roughly proportional to the magnitude of the spin signal that could be detected. A typical radical concentration, as measured by comparison with a standard sample of diphenylpicrylhydrazyl, was of the order of 10^{15} spins per milligram of doped phthalocyanine (about 1 radical per 1000 phthalocyanine molecules). When the doped samples were illuminated at room temperature with light absorbed in the long-wave-length band of phthalocyanine (6800 A), an increase in conductivity could be observed. Room-temperature illumination at shorter wave lengths (~4500 A) produced a decrease in conductivity. The ratio of the magnitudes of the "reverse" photoeffect (i.e., the decrease in conductivity caused by 4500 A light) and the normal phthalocyanine photoconductivity (i.e., the increase in conductivity caused by 6800 A light) increases with the extent of doping. The action spectrum of the reverse photoeffect obtained with a heavily doped sample is shown in Fig. 11. The significance of this action spectrum is not unambiguous, inasmuch as it probably represents the resultant of two opposing processes.

When the doped samples were illuminated with white light at room temperature in the electron-spin resonance apparatus, a photoinduced

[7] D. Kearns and M. Calvin, in Bio-Organic Chemistry Quarterly Report, UCRL-8457, Sept. 1958, p. 25.

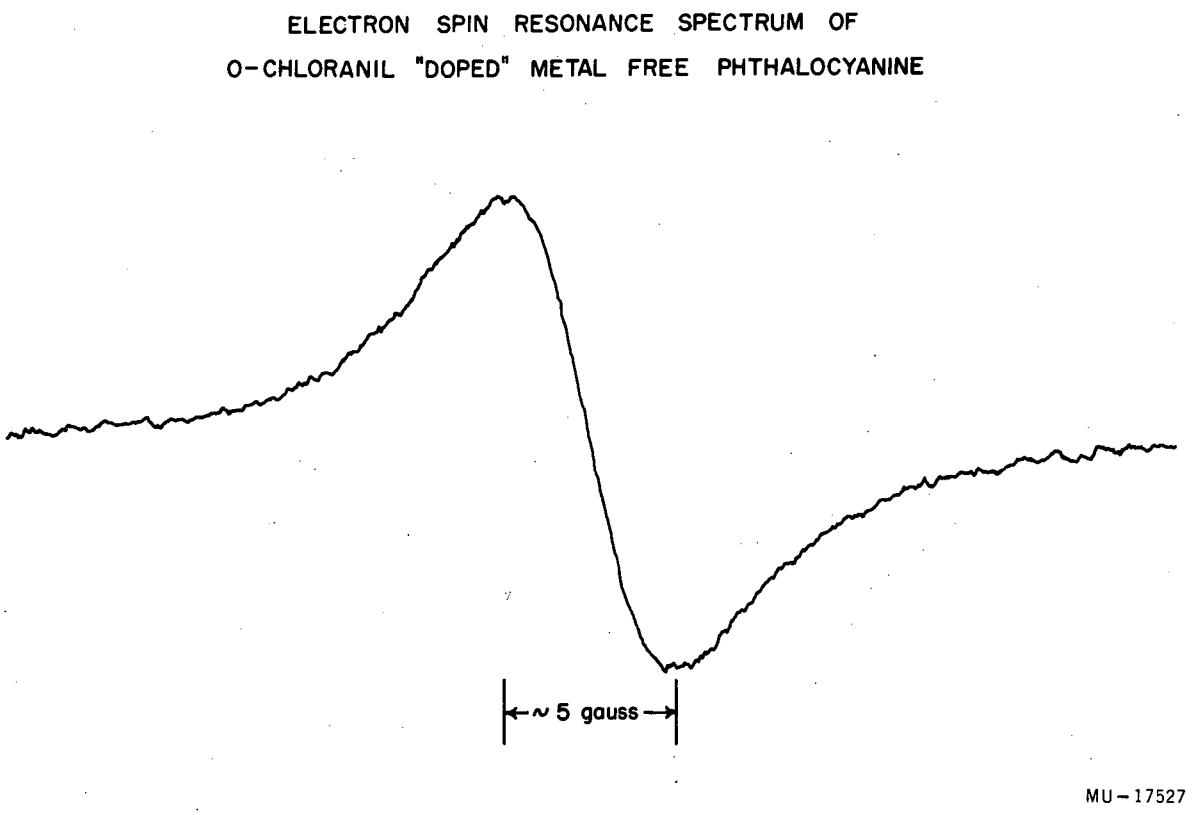

Fig. 10. Electron-spin-resonance spectrum of metal-free phthalocyanine "Doped" with o-chloranil.

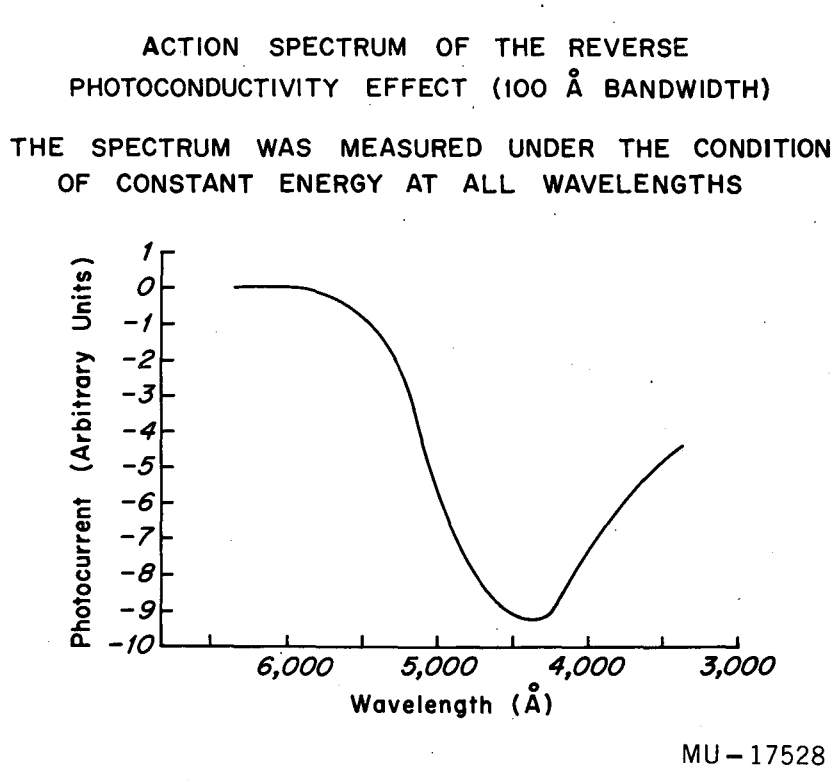

Fig. 11. Action spectrum of the reverse photoconductivity effect (100 Å band width). The spectrum was measured under the condition of constant energy at all wave lengths.

decrease in spin signal could be observed (see Fig. 12).

The room-temperature photocurrent-decay curves of doped samples upon flash illumination with wave lengths absorbed by phthalocyanine (6800 A) were essentially identical with the curves obtained with undoped samples at room temperature in the presence of high-intensity ambient light. This indicates that the carriers produced by doping behave in the same manner as photoproduced carriers in undoped material.

If the temperature of a doped sample was decreased from 23°C to -35°C, the dark current was decreased by several orders of magnitude, although it was still significantly above the room-temperature dark current for undoped samples. On the other hand, the photocurrent produced by light absorbed by phthalocyanine was greatly increased whereas the reverse photoeffect produced by 4500 A light was decreased by approximately the same factor.

At -35°C, the ratio of the photocurrent in doped samples to that in undoped samples was, under identical conditions, approximately 2000 to 1. The significance of this difference in terms of quantum efficiencies is discussed below.

D. Conclusions

The fact that the rise time of flash-induced photoconductivity is limited by the rise time of the flash (~ 1 microsecond) indicates that the electronically excited state which gives rise to charge carriers has a lifetime of less than 1 μsec. This immediately suggests the first excited singlet state, inasmuch as one would expect the lowest triplet state to have a much longer lifetime (of the order of 10^{-4} sec or more).[8]

The first 10 μsec of the photocurrent decay are complicated by the decay of the light pulse itself and therefore no attempt is made to discuss this region in any detail.

It was noted above that the photocurrent from 20 μsec to several hundred microseconds after flashing decayed significantly more slowly than would be predicted by the proposed mechanism, and that this effect became ever more pronounced and lasted for a longer time at lower flash intensities. This suggests that there exists a long-lived high-energy intermediate (of the order of 10^{-4}sec) which contributes to carrier production, but to a smaller extent than does the excited singlet state. One possiblility for such an intermediate is the lowest triplet state. Such an hypothesis would be consistent with the low-intensity-flash behavior of the current decay, inasmuch as the triplet lifetime would be longer under low-intensity illumination owing to a decreased probability of self-quenching.

The next question that arises is the detailed mechanism for the conversion of nonconducting excited electronic states into charge carriers.

[8] G. Porter and M. R. Wright, Disc. Faraday Soc., in press.

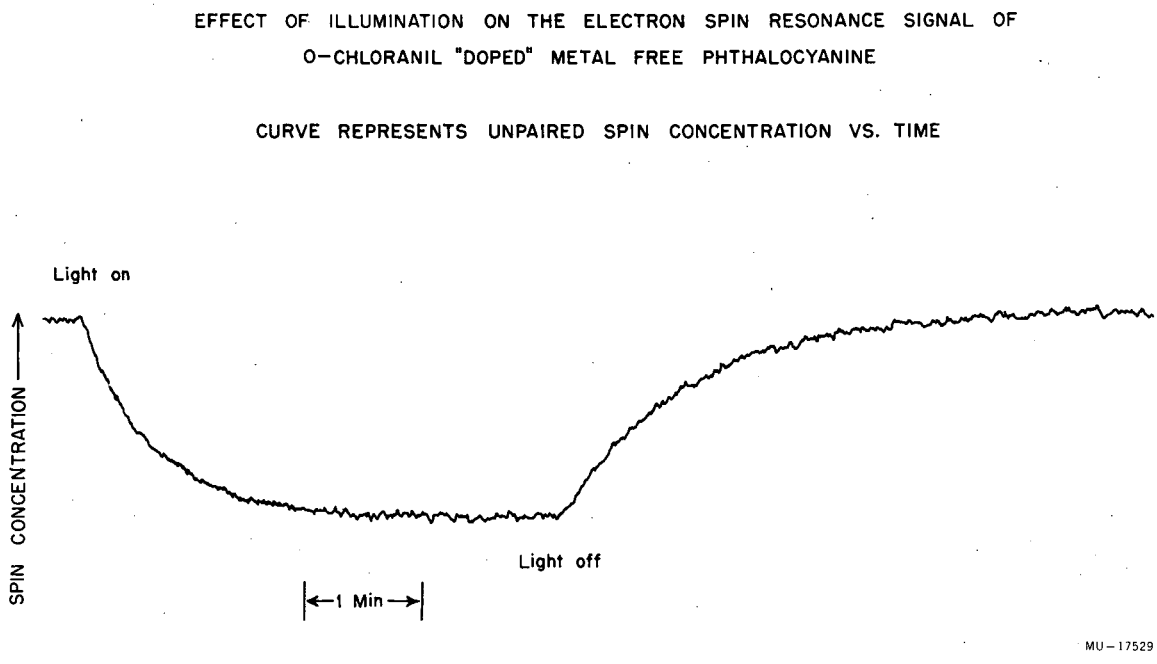

Fig. 12. Effect of illumination on the electron-spin-resonance signal metal-free phthalocyanine "Doped" with o-chloranil. Curve represents unpaired-spin concentration vs time.

It is possible to gain some insight into this problem by a consideration of the results of the doping experiments.

The phenomena exhibited by doped material may be most simply interpreted in the following manner. Ortho-chloranil is known to be a strong oxidizing agent and therefore might be expected to have a tendency to remove electrons from the metal-free phthalocyanine if the two substances were placed in intimate contact. The relative ease of transfer of electrons from the phthalocyanine to the ortho-chloranil would depend upon the electron affinity of ortho-chloranil and the ionization potential of phthalocyanine. It is postulated, then, that such an electron transfer takes place in the dark in the doped samples. Positives holes are thereby formed in the phthalocyanine layer which conduct electricity and give rise to the large dark currents. As noted above, the increases in the dark conductivity of phthalocyanine by doping was essentially linear with the number of free radicals produced. One may presume, then, that the free-radical concentration as measured by electron spin resonance would be approximately equal to the number of holes that could conduct current. These holes should behave in the same manner as holes produced by light in undoped samples. This is verified by the shape of the decay curve in doped materials (see Section 9).

From the fact that cooling reversibly decreases the dark conductivity of doped materials, it is possible to conclude that there is an activation energy for the electron transfer from phthalocyanine to ortho-chloranil and that the electron transfer is reversible.

The photoinduced decrease of room-temperature conductivity produced by 4500 A light indicates that the thermally induced electron transfer may also be reversed by light. This is further substantiated by the light-induced decrease of room-temperature electron spin resonance.

The 2000-fold increase in phthalocyanine photoconductivity at -35°C upon doping indicates that the presence of electron acceptors in the host lattice greatly increases the probability of conversion of light energy into charge carriers (see below for further discussion).

The above considerations suggest a possible mechanism for photoconductivity in undoped phthalocyanine (and, by analogy, in other organic dye materials). The essential feature of such a mechanism would involve a photoinduced electron transfer from the host material to either an oxidizing impurity in the lattice or to other host molecules, leading to the production of charge carriers.

On the basis of the proposed relationship between the number of unpaired spins as measured by electron spin resonance and the number of charge carriers (see above), it is possible to calculate a charge-carrier mobility for doped phthalocyanine by means of the relationship

$$I = \mu n E A. \tag{24}$$

This gives a value for the room-temperature mobility of 10^{-4} cm^2 per volt per second. Because of the errors inherent in the method used to measure the spin concentration, this value must be considered as accurate only within an order of magnitude (and probably too low rather than too high).

It must now be asked whether or not this calculated mobility represents the carrier mobility in undoped phthalocyanine. If the following assumptions are valid, then this identification may be made:
(a) The concentration of free radicals is a true measure of the concentration of free charge carriers. This assumption depends upon the validity of the mechanism for the increased dark conductivity of doped samples.
(b) The free charge carriers produced by doping are indistinguishable from those produced by light. The validity of this assumption is strongly supported by the observation that the carriers produced by doping cause the same effect on flash photoconductivity as does high-intensity ambient light in undoped samples.
(c) The mobility of charge carriers is unaffected by doping. The experiments quoted above demonstrated that doping produces charge carriers. Thus, the large increase in dark current caused by doping cannot be due solely to an increase in the mobility of the charge carriers already present in the undoped material. However, it is not possible at present to completely rule out a small effect of doping upon mobility.

It is of interest to compare the mobility given above with those obtained in inorganic semiconductors such as germanium and silicon. These latter normally range from 1 to 1000 cm^2 per volt per second at room temperature. Therefore, a value of 10^{-4} cm^2 per volt per second for an organic material is in keeping with the large differences between the crystal interactions in valence crystals and those in organic molecular crystals. For example, heats of sublimation are about 3 to 4 ev for valence crystals and about 10^{-2} ev for molecular crystals.

From the calculated mobility it is possible to measure a quantum yield for production of charge carriers by light in doped phthalocyanine. This yields a value of the order of unity. Therefore, if the above assumptions are correct, one obtains for undoped phthalocyanine a quantum yield of 5×10^{-4} for charge-carrier production by light. If Assumption (c) above is not entirely valid, the quantum yield for undoped material may be somewhat larger or somewhat smaller than 5×10^{-4}. However, it is still significantly less than unity.

Regardless of the absolute validity of the mobility and quantum yields quoted above, it is possible to state unequivocally that, under appropriate conditions (i.e., the presence of electron-accepting impurities), the quantum yield for charge-carrier production in organic materials can be greatly increased. This possibly has enormous significance for biological systems, particularly those involved in photosynthesis, where it is known that highly polarizable organic molecules (chlorophyll) exist in an ordered array, possibly in contact with strong electron acceptors (pyridine nucleotides, coenzyme Q, etc.), and where other evidence has suggested a "semiconductor" type of mechanism for the primary process.[1]

QUANTUM YIELD OF PHOTOINDUCED UNPAIRED ELECTRONS IN SPINACH CHLOROPLASTS

Lou Ann Carter and Power B. Sogo

The kinetics of the rise and decay of the photoinduced electron-spin-resonance (ESR) signal in plant material have been reported in previous papers.[1,2] We have measured the quantum efficiency for the production of the unpaired electrons that give rise to the ESR absorption. A value of 0.03±.02 has been obtained for the ratio of the number of unpaired electrons produced to the number of incident light quanta.

The experimental arrangement has been described in a previous paper. The method that was used for these experiments follows. The wave length of the incident light was restricted to a band about 400 A wide centered at about 7350 A by a combination of band-pass interference filters and a Corning infrared filter. The incident light intensity was measured with a bolometer which had been calibrated by a standard lamp. The 300-watt tungsten-filament projection lamp, filters, and condensing optics that were used gave a mean intensity of 1.1×10^{16} quanta/sec into the microwave cavity. The fraction of this light in the cavity that reached the sample was estimated to be 70% by the actinometer involving the photolysis of uranyl oxalate.[3] An ultraviolet source was substituted for the tungsten lamp for this calibration.

The ESR spectrometer was set to monitor the height of the signal, and change in height was recorded when the light was admitted. A known number of light quanta was injected by a calibrated camera shutter set for 1/5 sec. From the known shape of the curve for the light-induced signal in the steady state and a subtraction of the dark signal, we were able to obtain a curve corresponding to the light signal produced by the flash of light. This signal was compared to the signal arising from a sample containing 8 λ of 10^{-3} M Mn^{++} ions in aqueous solution. The Mn^{++} sample was taped to the silver-plated sample rod and the chloroplasts painted on the remainder of the exposed rod so that the two spectra could be obtained simultaneously.

The wave length of 7350 A was found to be the most favorable one for obtaining a reproducibly high quantum efficiency under the conditions of this experiment. For example, 6800 A gave a quantum efficiency only about 1/100 that for 7350 A. The interpretation of this result is not clear at present, and this wave-length dependence is currently being investigated.

---

[1] Barry Commoner, John J. Hise, and others et al., Science 126, 57 (1957).

[2] Power B. Sogo, Ning Pon, and Melvin Calvin et al., Proc. Nat. Acad. Sci. 43, 387 (1957).

[3] Daniels, Mathews, and Williams, Experimental Physical Chemistry, (McGraw-Hill, New York, 1956).

THE HILL REACTION AND $C^{14}O_2$ FIXATION IN INTACT, WASHED, AND FRAGMENTED CHLOROPLASTS

Roderic B. Park, Karel P. Louwrier, and Ning G. Pon

Many photosynthetic cells evolve oxygen in the presence of light and water when an artificial oxidant is substituted for CO_2.[1] This reaction is called the Hill reaction, and, if the oxidant is $K_3Fe(CN)_6$, it may be formulated as

$$2\,Fe(CN)_6^{-3} + H_2O \xrightarrow[\text{photosynthetic material}]{\text{light}} 2\,Fe(CN)_6^{-4} + 2\,H^+ + 1/2\,O_2 \uparrow .$$

Since the light energy needed to drive this reaction is absorbed by chlorophyll,[2] and since oxygen evolved by the reaction arises from water,[3] it is generally conceded that the Hill reaction is analagous to the natural photochemical processes of photosynthesis. Both intact and fragmented cells carry out the Hill reaction. Centrifugal fractionation of fragmented cells from a wide variety of tissues has shown that Hill-reaction activity is localized within the chlorophyll-containing plastids (chloroplasts) of photosynthetic tissues.

Jagendorf has noted that the Hill-reaction activity of chloroplasts is increased when they are removed from an isotonic medium and are suspended in a dilute NaCl solution.[4] Under these conditions a chloroplast swells and a chloroplast swells and a chloroplast surface membrane might be expected to become porous, allowing the oxidant used in these experiments (ferricyanide) to penetrate the chloroplast more rapidly. Previous work in this laboratory has shown that the Hill-reaction rate of isolated spinach chloroplasts, on a unit chlorophyll basis using ferricyanide as the oxidant, is increased as much as fivefold when the chloroplasts are sonically fragmented.[5] Both Jagendorg's and our own observations indicate that the intact chloroplast is surrounded by a diffusion barrier with respect to ferricyanide ion.

Arnon[6] and Holm-Hansen[7] have studied $C^{14}O_2$ fixation in intact chloroplasts and have shown that the fixation products are similar to

---

[1] R. Hill and R. Scarisbrick, Proc. Roy. Soc. (London) B. 129, 238 (1940).

[2] S. L. Chen, Plant Physiol. 27, 35 (1952).

[3] A. S. Holt and C. S. French, Arch. Biochem. 19, 429 (1948)

[4] M. Avron, D. W. Krogmann, and A. T. Jagendorf, Biochim. Biophys. Acta 30, 141 (1958).

[5] R. B. Park and N. G. Pon, in Bio-Organic Chemistry Quarterly Report, UCRL-8575, Dec. 1958, p. 27.

[6] Arnon, Allen, and Whatley, Biochim. Biophys. Acta 20, 462 (1956).

[7] O. Holm-Hansen, V. Moses, K. Nishida, N. Pon, and M. Calvin, Physiologia Plantarum (in press).

the photosynthetic fixation products found in algae. To obtain the maximum $C^{14}O_2$ fixation rate in chloroplasts it was necessary to add a variety of enzymatic cofactors. The possibility exists that as chloroplast rupture enhances Hill reaction activity, it may also enhance $C^{14}O_2$ fixation by removing a permeability barrier for some of the necessary cofactors which increase $C^{14}O_2$ fixation by chloroplast systems.

To test such a possibility we performed the following experiment. Chloroplasts were prepared according to the flow sheet in Fig. 13. The three preparation--whole, washed and sonically fragmented chloroplasts--contained the same amounts of chlorophyll, and differed principally in their states of aggregation. The Hill-reaction activity of these preparations is given in Table I. In a similar experiment the intact, washed, and sonically fragmented chloroplasts were incubated for 30 minutes with C^{14}-bicarbonate in light and dark experiments. The results from the $C^{14}O_2$ fixation experiments are also given in Table I.

The increase in Hill reaction rate and in $C^{14}O_2$ fixation rate with decreasing organization of the chloroplast suggests the presence in intact chloroplasts of a permeability barrier to one or more of the cofactors or substrates for these reactions. It has already been suggested that ferricyanide permeability is the rate-limiting process in Hill reaction of whole chloroplasts. Permeability studies on a number of biochemical systems have shown that phosphorylated organic compounds are often unable to penetrate biological membranes in the phosphorylated form. If the chloroplast is surrounded by such a membrane, several of the phosphorylated cofactors may be unable to penetrate the intact chloroplast readily. Experimental support for such a notion is available from the work of Tolbert,[8] who has shown that C^{14}-labeled phosphate esters cannot be removed from intact Swiss chard chloroplasts by washing with 0.5 M sucrose or 0.35 M NaCl. A water or methanol wash ruptures the chloroplasts and releases the photosynthetic intermediates. Presumably this permeability barrier would also prevent diffusion of cofactors into the chloroplast. Because of the permeability problems associated with intact and washed chloroplast, most of our experiments on $C^{14}O_2$ fixation and the Hill reaction in chloroplasts are now being carried out in sonically fragmented systems.

[8] N. E. Tolbert, The Photochemical Appartus: Its Structure and Function, Brookhaven National Laboratory Biology Conference, Number 11 (June, 1958), Report No. BNL-512 (C28), 1959, p. 271.

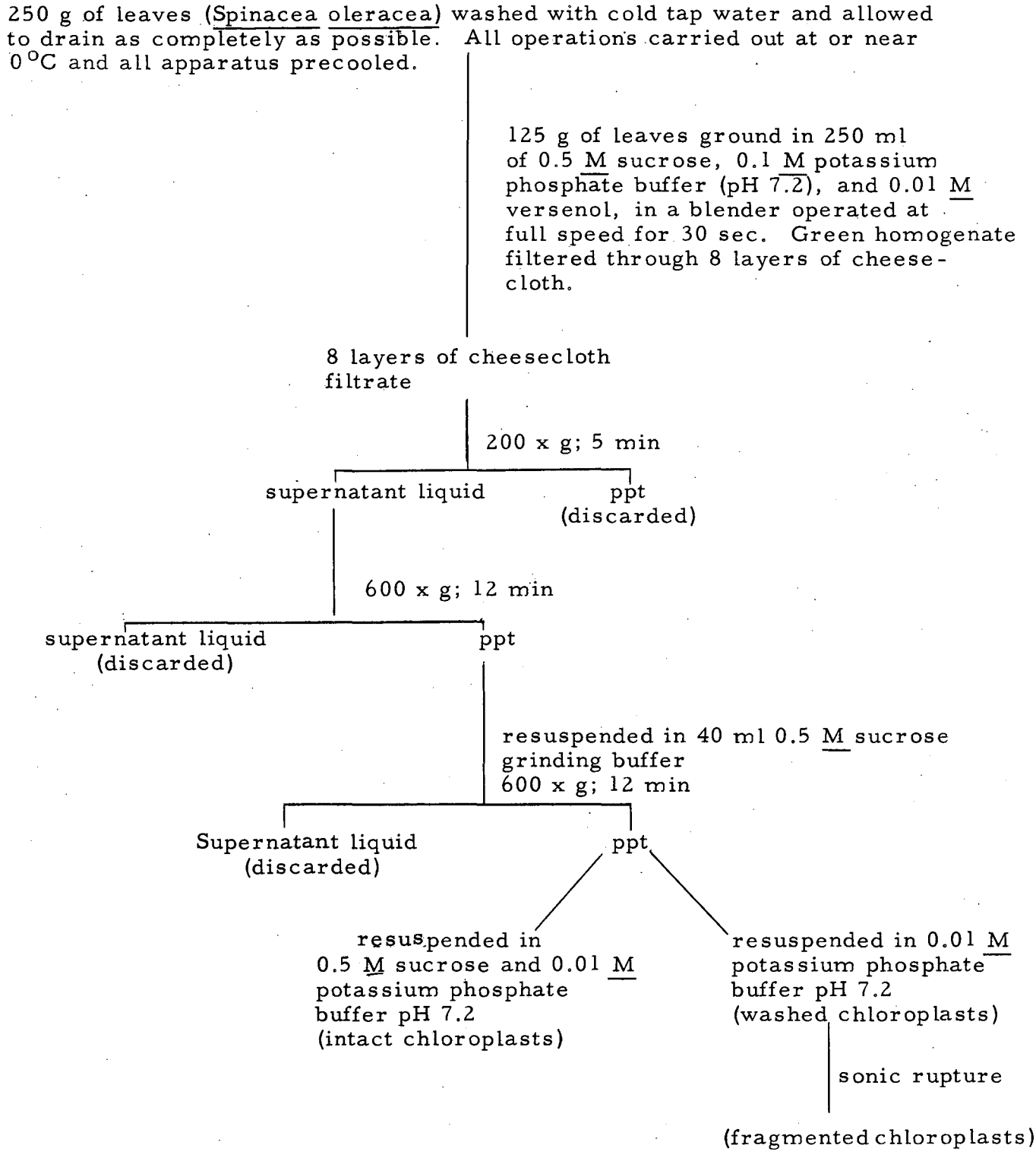

Fig. 13. Flow sheet for preparation of intact, washed, and sonically fragmented chloroplasts.

Table I

Hill-reaction activity and $C^{14}O_2$ fixation activity of intact, washed, and sonically fragmented spinach chloroplasts

Type of Chloroplast	$C^{14}O_2$ Fixation[a] (Cpm/mg chlorophyll)		Hill reaction[b] (O_2 evolved in λ/hr/mg chlorophyll)
	Light	Dark	
Intact	530,000	50,000	265
Washed	1,600,000	39,000	305
Fragments	2,300,000	40,000	460

[a]Each reaction mixture contained 0.2 μM triphosphopyride nucleotide, 0.24 μM diphosphopyridine nucleotide, 1.6 μM thiamine pyrophosphate, 1.2 μM adenosine-5'-triphosphate, 3.0 μM ascorbate, 4.8 μM $MgSO_4$, 2.4 μM $MnCl_2$, 1.7 μM $HC^{14}O^-$ (40 μC), and 1 ml chloroplast suspension containing 1.25 mg chlorophyll. Reaction mixtures were incubated 30 min at 20°C.

[b]Oxygen evolution determined manometrically at 20°C. Each Warburg flask contained 2.8 ml of chloroplast suspension (2 mg chlorophyll) and 40 μM of $K_3Fe(CN)_6$.

BIODYNAMICS OF CARBON REDUCTION DURING PHOTOSYNTHESIS

J. A. Bassham and Martha R. Kirk

Studies of the fixation and reduction of carbon dioxide during periods of steady-state photosynthesis, in which C^{14} is employed as a tracer element,[1,2] are being continued. These studies are to determine the qualitative features of various carbon-reduction pathways (identity and sequence of intermediate compounds), and to obtain information on certain dynamic aspects of the metabolic network as it operates in vivo. Among these aspects are the following:

(a) The concentrations of intermediates during steady-state photosynthesis under selected environmental conditions;

(b) the net rates for conversion of each intermediate compound to the next intermediate in a given pathway;

(c) the ratio of forward- to back-reaction rates in each step, and the steady-state free-energy change to which this ratio is directly related;

(d) the relative contribution, in terms of net flow of carbon, of each of the various pathways, and a quantitative comparison of these contributions with the externally measured rates of uptake of carbon dioxide; and

(e) the effects of changes in various environmental factors on each of the above quantities.

Taken together, these and other dynamic factors of the in vivo metabolic network constitute what we shall call the "biodynamics" of the system.

Several improvements in the apparatus used for steady-state studies of photosynthetic carbon reduction as described in previous reports have been made. A diagram of the apparatus in current use is shown in Fig. 14. One of the problems has been the maintenance of constant pH in the algae suspension during the course of the experiment without resorting to buffer concentrations which would make impossible the subsequent chromatographic analyses of samples of the algae. If ammonium salts are used in the nutrient medium as a source of nitrogen for the algae, the suspension becomes more acidic as the algae exchange hydrogen ions for ammonium ions. If nitrate salts are used, the algae suspension becomes more alkaline with time. This problem has been solved by installation of pH electrodes in a side loop of the vessel containing the algae. The algal suspension is circulated through this loop by the flow of gas into the vessel through one end of the loop. The signal from the pH meter connected to the pH electrodes is fed to a control relay which may be set for the desired pH. The control relay actuates a small valve which admits dilute NH_4OH or HNO_3 to the algal suspension whenever the pH tends to change from the set value. If nitrogen is supplied initially to the algae in the form of nitrate, the pH tends to increase, therefore dilute nitric acid is placed in the reservoir.

---

[1] J. A. Bassham, M. Kirk, and T. Andrews, in Bio-Organic Chemistry Quarterly Report, UCRL-8698, March 1959, p. 19.

[2] J. A. Bassham, and M. Kirk, in Bio-Organic Chemistry Quarterly Report, UCRL-8421, June 1958, p. 18.

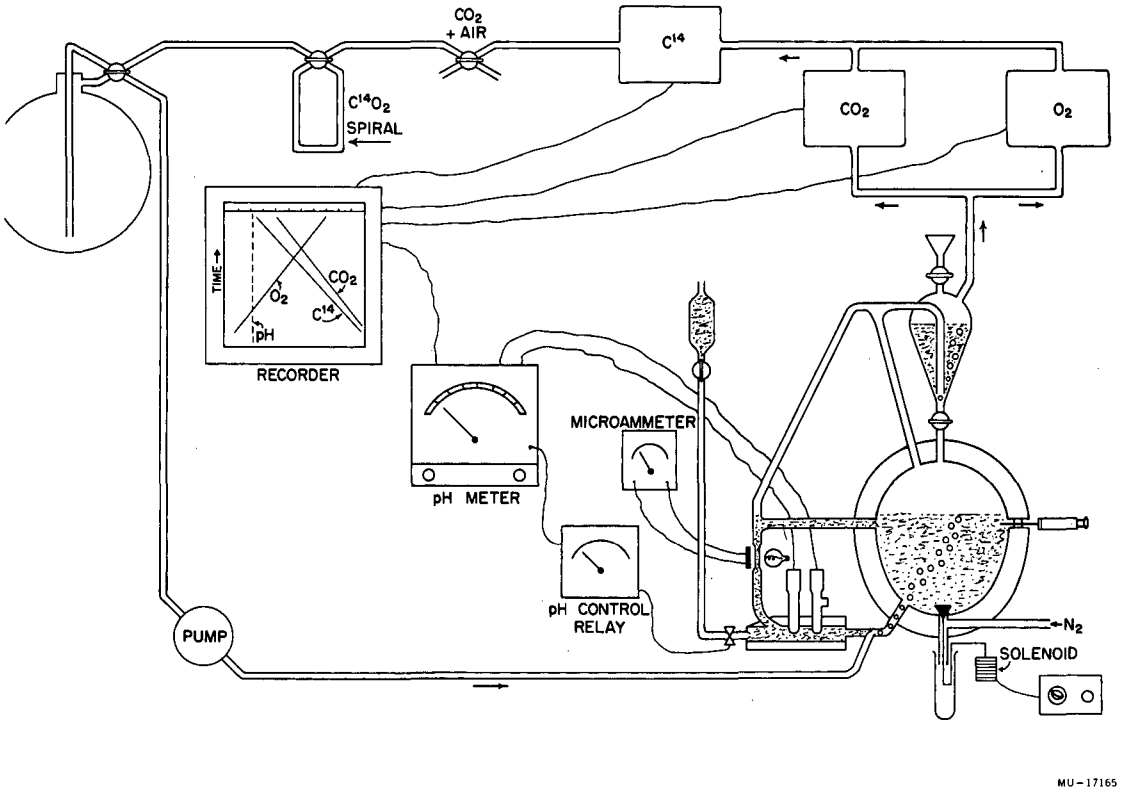

Fig. 14. Apparatus for steady-state photosynthesis studies.

By using known ratios of nitrogen requirements to other inorganic mineral requirements, one can add to the solution of dilute nitric acid or ammonium hydroxide some of the other minerals that would be used up by the algae as the nitrate or ammonia is taken up. In this way it is possible to begin the experiment with a very dilute nutrient solution and yet be certain that minerals are present during the course of the experiment in the concentrations required for steady-state photosynthesis.

Another improvement in the apparatus is the addition of a solenoid-operated sampling valve which permits the taking of samples of algal suspension of uniform size (about one ml) with great rapidity (every 2 sec) after introduction of C^{14} to the algae.

In order to insure that at the start of the labeling period the specific activity of the carbon dioxide changes from zero to its final value in 2 or 3 sec, it is necessary (in addition to turning the stopcock to admit $C^{14}O_2$) to inject directly into the algae suspension an amount of $HC^{14}O^-_3$ which is calculated to at once bring the specific activity of the dissolved CO_2 and bicarbonate ion to the same specific activity as the gas phase.

The appartus, as just described, has been used in several experiments. In the most recent experiment, a good agreement between externally measured CO_2 uptake and the rate of labeling of compounds of the carbon-reduction cycle and related compounds has been obtained. This correlation is shown in Table II.

During the first 15 sec, the rate of appearance of C^{14} in soluble compounds on the paper chromatograms (Fig. 15) is less than the maximum rate, owing perhaps to a reservoir of unlabeled carbon dioxide and bicarbonate in the algal cells at the beginning of the experiment. The difference between (a) the curve of total C^{14} in compounds on the paper between 18 and 32 sec and (b) a line of the same slope drawn through the origin is indicative of the size of this reservoir, about 1 to 1.5 μmoles of C. After 32 sec, the rate again falls off because by that time an appreciable amount of the C^{14} taken up has found its way into insoluble compounds not seen on the chromatogram.

As a result of this experiment, it can be stated unequivocally that the carbon-reduction cycle or a pathway involving the same compounds[3] accounts for at least 85% of all the carbon incorporated during photosynthesis, under the conditions of this experiment.

In the same experiment, the rates of appearance and the saturation level of radiocarbon in the various individual compounds of the carbon-reduction cycle and in many compounds derived directly from the cycle have been carefully determined. Some typical labeling and saturation curves of these data are shown in Fig. 16. It may be seen that the sugar phosphates and phosphoglyceric acid saturate in 2 to 5 minutes. The sugar

[3] Bassham, Benson, Kay, Harris, Wilson, and Calvin, J. Am. Chem. Soc. 76, 1760 (1954).

Table II

Comparison of externally measured CO_2 uptake with $C^{14}O_2$ Reduced by Algae

Quantity measured	Amount (μmoles/min/ml wet packed algae)
CO_2 uptake, measured externally	14 to 15
C^{14} uptake, measured externally[a]	14 to 15
C^{14} incorporated into algae samples, count of algae-alcohol mixture[a]	15
C^{14} found in soluble compounds on paper chromatogram, max. rate (18 to 32 sec)[a]	13

[a]Carbon-14 readings converted to μmoles of carbon by dividing actual measured radioactivity by specific radioactivity as measured during the course of experiment by CO_2 analyzer and ionization chamber (Fig. 14).

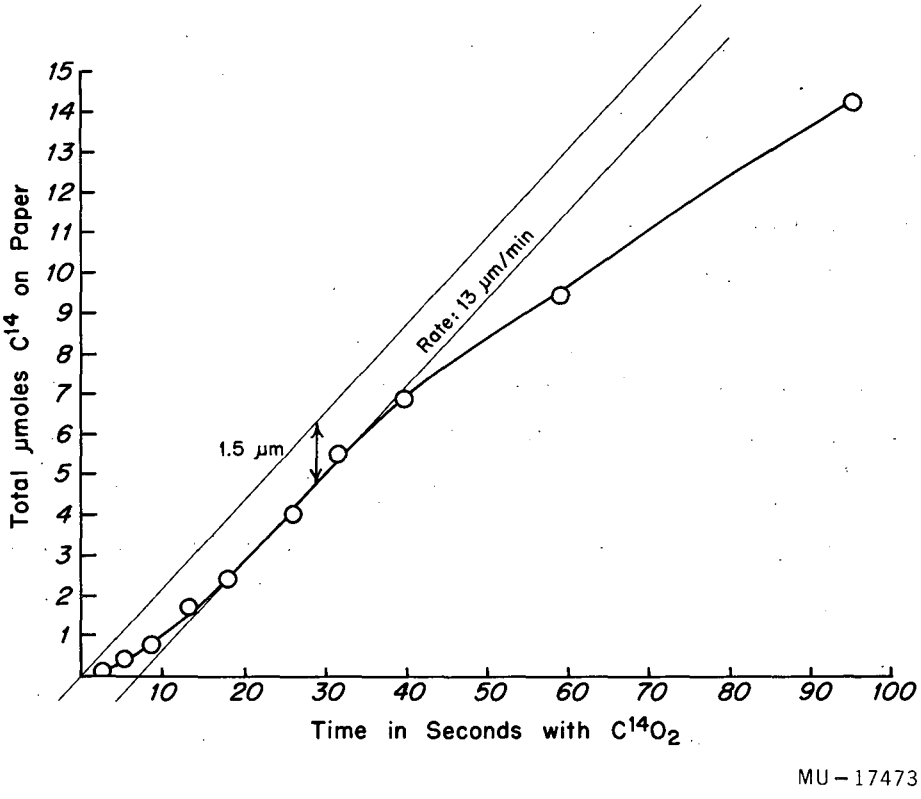

Fig. 15. Total radiocarbon found in all radioactive compounds on paper chromatograms from steady-state photosynthesis experiment.

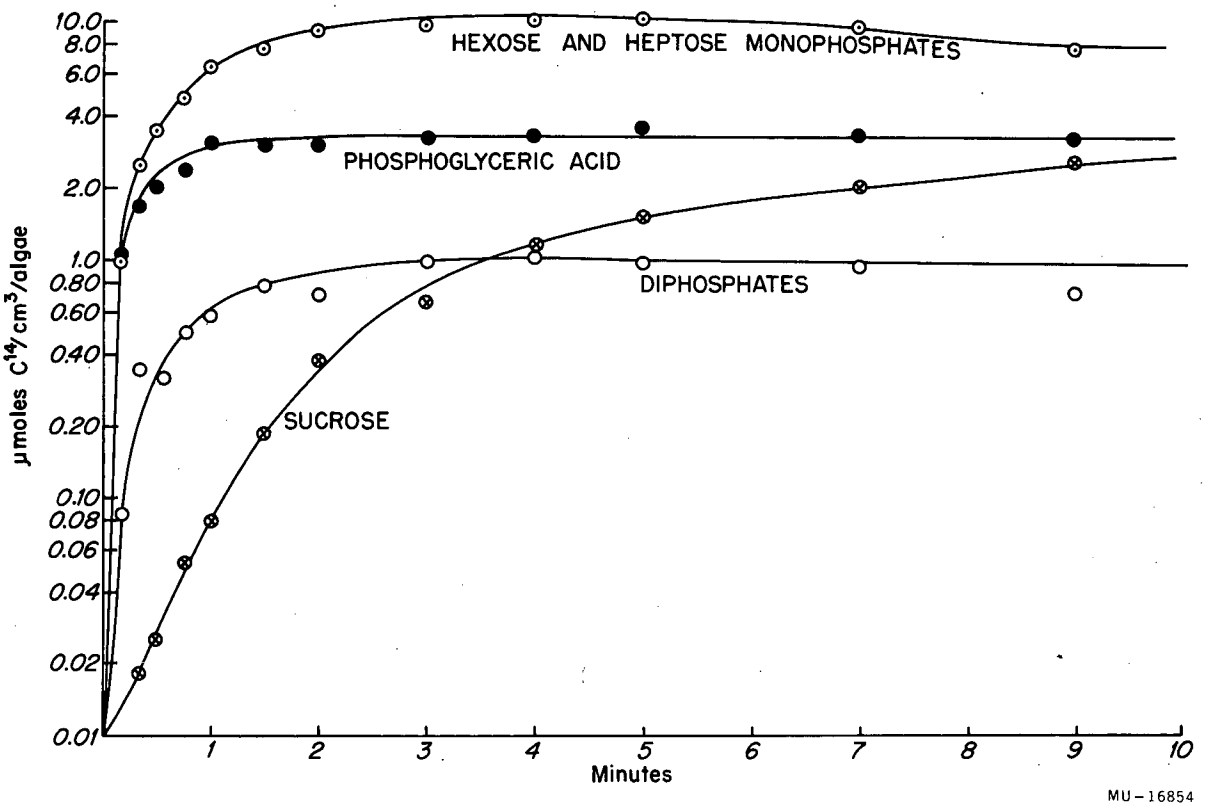

Fig. 16. Appearance of radiocarbon as a function of time of steady-state photosynthesis in PGA and sugar phosphate.

monophosphates and sugar diphosphates have been eluted, subjected to phosphatase, and rechromatographed. The individual labeling and saturation curves for these compounds have been determined and are much like the curves shown. The apparent slowness of the total sugar monophosphate curves to saturate probably is due to the labeling of mannose phosphate, not in the cycle.

The ribulose diphosphate curve has much the same shape and saturation time as the PGA curve. It is of interest to see if something about the mechanism of the carbonxylation of the carbon-reduction cycle may be learned from these data. As the cycle has usually been written,[3] the carboxylation of ribulose diphosphate results in the formation of two molecules of 3-phosphoglyceric acid. In this case one of the two carboxyl carbon atoms produced each time would be derived directly from the CO_2 incorporated in the reaction. The other five carbon atoms (PGA "residue") of the two molecules of PGA produced would all be derived from the ribulose diphosphate. Therefore, if this reaction is correctly formulated, the average specific radioactivity of these five "residual" carbon atoms of PGA should be no greater at any time than the average specific radioactivity of the ribulose diphosphate.

From time to time, the possibility has been suggested that the carboxylation of ribulose diphosphate might lead to only one molecule of PGA, containing the carboxyl derived directly from CO_2, and one molecule of some other three-carbon compound not in rapid equilibrium with the PGA pool.[4] In this case, the two other carbon atoms of the single PGA molecule would be derived from ribulose diphosphate, probably from carbon atoms Numbers 1 and 2. Thus the average specific radioactivity of the two "residual" PGA carbon atoms would not necessarily follow the specific radioactivity of the ribulose diphosphate molecule as a whole.

The concentration of carbon in PGA in this experiment is 3.0 μmoles/ml wet-packed algae, so that the total carboxyl concentration is 1.0 μmole. In the first proposed carboxylation reaction (→2 PGA), the carboxyl carbon derived directly from CO_2 would then represent only 0.5 μmoles. Since the rate of flow of C^{14} through this carboxyl is 12 μmoles/min it will saturate very quickly. In fact, even allowing for the CO_2 pool in the algae, the carboxyl derived from CO_2 will be saturated after 30 sec, and the degree of saturation has been calculated for times shorter than 30 sec. This calculation has been made (Table III) for a reaction leading to one PGA molecule and for a reaction leading to two PGA molecules. These levels of carboxyl carbon have been subtracted from the total labeling of the PGA for various times of photosynthesis, and the resulting calculated labeling of the PGA "residue" is compared with the labeling of ribulose diphosphate (Table IV).

It can be seen that the result agrees best with the reaction leading to only one molecule of PGA, since in the reaction giving two PGA molecules the specific radioactivity of the PGA "residue" precedes the specific radioactivity of ribulose diphosphate.

---

[4] A. T. Wilson and M. Calvin, J. Am. Chem. Soc. 77, 5948 (1955).

Table III

PGA carboxyl (from CO_2) saturation

Reaction 1: CO_2 + RuDP → 2 PGA

Reaction 2: CO_2 + RuDP → PGA + C_3

Assuming CO_2 in algae reservoir = 1.0 μmole/cc, algae rate CO_2 into PGA = 12.0 μmole/min/cc algae.

	Reaction 1		Reaction 2	
Time (sec)	% saturation	μmoles C^{14}	% saturation	μmoles C^{14}
2.5	1.3	0.067	8	0.08
5.0	31	0.157	24	0.24
8.5	52	0.27	48	0.48
13	72	0.37	71	0.710
18	86	0.43	86	0.86
26	92	0.47	94	0.94
31.5	93	0.48	97	0.97
40	100	0.50	98	0.98
59		0.5	100	1.0

Table IV

% Saturation (= K x specific activity)

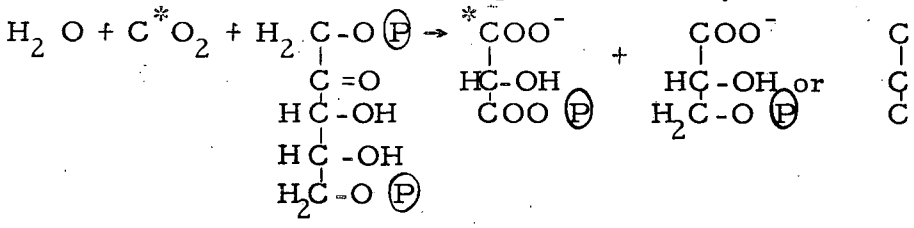

Time (sec)	PGA	PGA-$\frac{COOH}{2}$	PGA-(COOH)	RuDP
8.5	15	8	0	7
13	25	15	2	11
18	33	22	7	14
26	46	36	22	23
40	64	57	47	44
90	87	84	80	72
180	95	94	92	88

$C^{14}O_2$ in: 12 μmole/min/cc algae PGA carboxyl: 1.00 μmole/cc algae

The appearance of radiocarbon in some compounds outside the carbon-reduction cycle, or "secondary intermediates," is shown in Fig. 17. It may be seen that many of these compounds become saturated with C^{14} after a few minutes under conditions of "steady-state" photosynthesis. This is in contrast to earlier experiments in this laboratory, in which frequently no nitrogen was supplied to the algae (either as nitrate or ammonia) and consequently amino acids and some related compounds were labeled more slowly. It is now possible to measure the concentrations of active reservoirs of these compounds.

The method of calculating the rate of passage of carbon through a given secondary intermediate compound, such as aspartic acid, depends on a determination of the number of "changes" of the carbon in the compound necessary to produce the measured degree of saturation at a given time. Suppose that at steady state, carbon is flowing through an intermediate compound A with a concentration of A_s µmoles at a rate of R µmoles per minute. Then the number of changes of carbon in the compound is A_s/R changes per minute. Let the entering carbon be suddenly labeled with C^{14} of constant specific radioactivity. The specific radioactivity of A, initially zero, begins to rise and follows an exponential function that levels off when A is at the same specific radioactivity as the entering carbon. Let the number of changes of A at any time be given by x and the degree of saturation of A be given by y, which is equal to the specific activity of A divided by the specific activity of the entering carbon. Then one has $y = 1 - e^{-x}$, a function shown in Fig. 18.

The value of y at any time may be calculated by dividing the radioactivity found in A at that time by the radioactivity found in A when it is saturated. From the values of y at several different times before saturation, the numbers of changes the compound has undergone during these times may be calculated:

$$y_1 = 1 - e^{-x_1} \text{ at } t_1,$$

$$y_2 = 1 - e^{-x_2} \text{ at } t_2 .$$

From this, $\frac{x_2 - x_1}{\Delta t} = \frac{x_2 - x_1}{t_2 - t_1}$ = number of changes per unit time, or $\Delta x/\Delta t$. Then the rate of carbon flow through the compound is given by $R = A_s \frac{\Delta x}{\Delta t} \frac{\mu\text{moles}}{\text{minute}}$. An example of this calculation is given in Table V.

Of course, this calculation is not valid until the precursor of the compound in question is saturated with radiocarbon. If the precursor is not saturated, the calculated rate of flow of carbon through the compound in question usually increases as the time from the start of the experiment

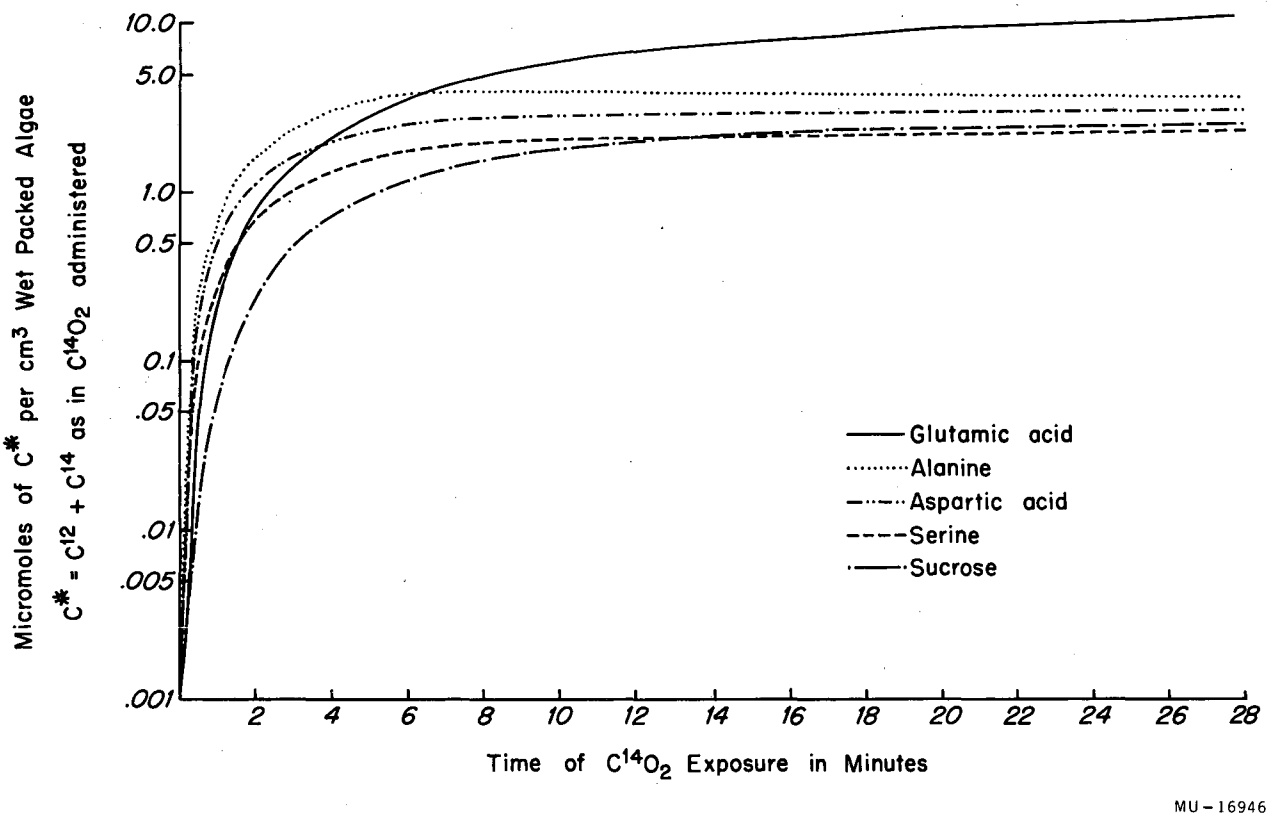

Fig. 17. Appearance of radiocarbon as a function of time of steady-state photosynthesis, in some secondary intermediate compounds.

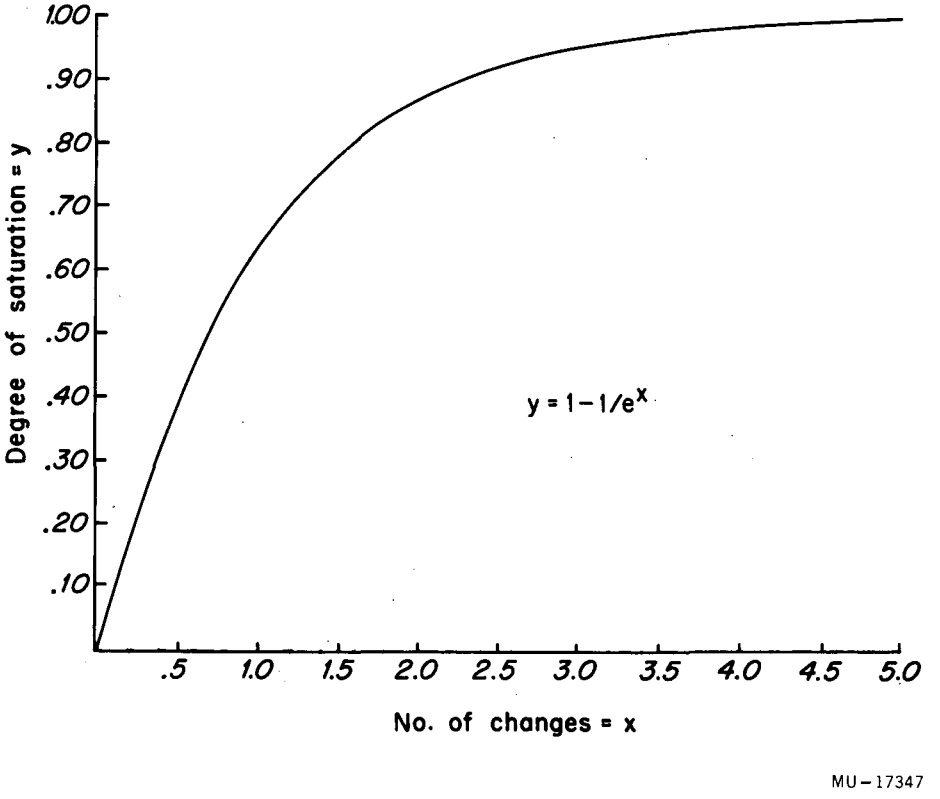

Fig. 18. Theoretical approach to saturation labeling of an intermediate compound as a function of number of changes of carbon.

Table V

Sample calculation: rate of flow of carbon through aspartic acid

time, t (min)	a, amount of C^{14} (μmoles)	y, degree of saturation	x, number of changes	Δx	change, $(a_s) \cdot \Delta x$ (μmoles)	rate $\frac{a_s \Delta x}{\Delta t}$ (μmoles/min)
3	1.06	0.35	0.39			
				0.35	1.05	0.52
5	1.59	0.53	0.74			
				0.92	2.76	0.55
10	2.42	0.81	1.66			
20 (a_s)	3.00					

increases. Once the precursor is saturated, the calculated rates from successive intervals become constant, as shown in the example.

Another assumption inherent in the above calculation is that the rates of the reverse reactions are small compared with the rates of the forward reactions, so that the rates of the forward reactions are essentially the rate of flow of carbon through the compound. This assumption is not always true. The validity of this assumption might be checked by calculating the steady-state free-energy changes of the reactions before and after the intermediate in the pathway and applying the equation

$$\Delta F^s = -RT \ln \frac{f}{b} ,$$

where ΔF^s = the free energy of the reaction at steady state, f = the rate of the forward reaction, and b = the rate of the back reaction. We have not yet made this calculation for secondary intermediates but, since we can measure the steady-state concentrations of intermediate compounds, we are in a position to make such a calculation wherever the standard free-energy changes are known.

The contribution of the carboxylation of three-carbon compounds (probably phosphoenolpyruvic acid) to give four-carbon compounds has been roughly estimated. The expected product of this carboxylation, oxaloacetic acid, is not seen on our chromatograms, owing to its instability, but malic acid and aspartic acid, believed to be derived from oxaloacetic acid, are among the labeled compounds seen on the paper chromatograms after very short exposures of the algae to C^{14}. Also seen at somewhat longer times are radioactive citric acid--which is presumed to be formed by a condensation of oxaloacetate with acetyl Coenzyme A--and glutamic acid--which may be formed by reductive amination of ketoglutaric acid, derived from the condensation product of oxaloacetate and acetyl Co A. The rates of passage of carbon into these compounds have been estimated by methods described above. By using the total rate of incorporation of C^{14} into these compounds, it is estimated that four-carbon compounds are formed at a rate of about 2.5 μmoles/min, although the rate may be somewhat higher if other compounds not included in this calculation are in fact formed by this route. Since three of the carbon atoms in this formation of four-carbon compounds come from the carbon-reduction cycle via PGA and phosphoenolpyruvic acid, this means that only about 0.6 μmole of CO_2 per minute per ml of algae is incorporated via this carboxylation. This would be about 5% of the total carbon dioxide fixation.

In conclusion, it may be said that methods have been developed to permit measurement of biodynamic properties of carbon transformation during photosynthesis and that these methods as they have been applied so far indicate that

(a) the carbon-reduction cycle of photosynthesis is responsible for 80% or more of all carbon dioxide fixed by the algae under the conditions used;

(b) the carboxylation reaction in vivo may lead to the formation of only one molecule of PGA and one molecule of some other three-carbon compound;

(c) the carboxylation of a three-carbon compound to give four-carbon compounds probably does not account for more than 5 to 10% of all the carbon dioxide incorporated.

PRELIMINARY INCUBATION STUDIES OF CARBOXYDISMUTASE

Ning G. Pon

Introduction

When carboxydismutase is preincubated with either Ni^{++} or Mg^{++}, some marked effects on its enzymic activity are observed. For example, preliminary incubation of the enzyme with Ni^{++} at 0°C and 25°C caused the activity of carboxydismutase to rise sharply to a maximum and, after reaching the peak, to decrease gradually as a function of preincubation time.[1] Preincubation of the enzyme with Mg^{++} at 0°C, on the other hand, yielded the same rapid rise of the activity, but no decrease of activity over the same period of preincubation.[2] Instead a gradual leveling off of the activity was observed. Further studies of the preliminary incubation of Mg^{++} at 25°C with carboxydismutase indicated that the maximum activity of the enzyme is reached after several seconds. From these data it was concluded that, of these two metal ions, Mg^{++} is the "true" cofactor for this enzyme system. Other metal ions, such as Mn^{++}, Co^{++} and Cr^{+++}, however, are known to activate carboxydismutase.[3,4] Until the effects of the preincubation of the enzyme with these metal ions are studied, the identity of the "true" cofactor remains uncertain. In this report, therefore, are described some studies with these metal ions as well as those with Mg^{++} and Ni^{++}.

---

[1] Ning G. Pon, in Chemistry Division Quarterly Report, UCRL-3595, Oct. 1956, p. 52

[2] Ning G. Pon, Brian R. Rabin, and Yasuo Natori, in Chemistry Division Quarterly Report, UCRL-8204, March 1958, p. 27.

[3] Ning G. Pon, in Chemistry Division Quarterly Report, UCRL-3361, March 1956, p. 50.

[4] Arthur Weissbach, B. L. Horecker, and Jerard Hurwitz, J. Biol. Chem. 218, 795 (1956).

Along with these investigations, the preliminary incubation of carboxydismutase with its substrates, bicarbonate and ribulose-1, 5-diphosphate (RuDP), was also studied. By experiments of this type it is possible that the nature of the activated complex can be deduced. In particular, it is hoped that the sequence of combination of metal ion and substrates with the enzyme to form the enzyme-metal-substrate complex can be elaborated.

Experimental Procedure

The detailed procedure for these experiments has been given elsewhere.[2] In these experiments there were two phases, (a) the preincubation step and (b) the incubation step. The former step consisted in mixing of all except one or two of the components of the carboxydismutase system and allowing this incomplete system to stand either at 0°C or 25°C for the required time. At the end of this period, the remainder of the components was added and the incubation was carried out at 25°C for a fixed time (usually 5 or 10 min). The reaction was stopped by the addition of acetic acid. A suitable aliquot portion of this mixture was plated and counted.

Lyophilized enzyme preparations, stored for about 2 years at -15°C, were used for these experiments. The enzyme was prepared by ammonium sulfate fractionation of the chloroplast extract of Tetragonia followed by dialysis and lyophilization.[5]

Results and Discussion

The results of the preliminary incubation of carboxydismutase with metal ions are shown in Fig. 19. A large effect is observed with Mg^{++} ion. Contrary to previous results,[1] Ni^{++} does not show any preincubation effect. In fact, Ni^{++}, Mn^{++}, and Co^{++} do not activate the enzyme at all. This negative result may be due to the presence of tris* as a buffer or due to the age of the enzyme, or both. (The formation of a metal-tris complex is evidenced by the change in color of the solution of metal ion when tris is added.) Some experiments carried out in the absence of tris show that after 10 minutes' preincubation with Ni^{++} at 0°C, the enzyme is indeed made more active, but, at best, only twofold. (Enhancement of activity in a fresh enzyme preparation by Ni^{++} under these conditions is routinely 50 to 100 times that of the control with no metal ions added.) The above results show that it is not yet possible to make any definite conclusions, but the data are at least consistent with the view that Mg^{++} is the "true" cofactor.

---

[5] Ning G. Pon and Brian R. Rabin, in Chemistry Division Quarterly Report, UCRL-3710, March 1957, p. 33.

*Tris: Tris (hydroxymethyl) aminomethane.

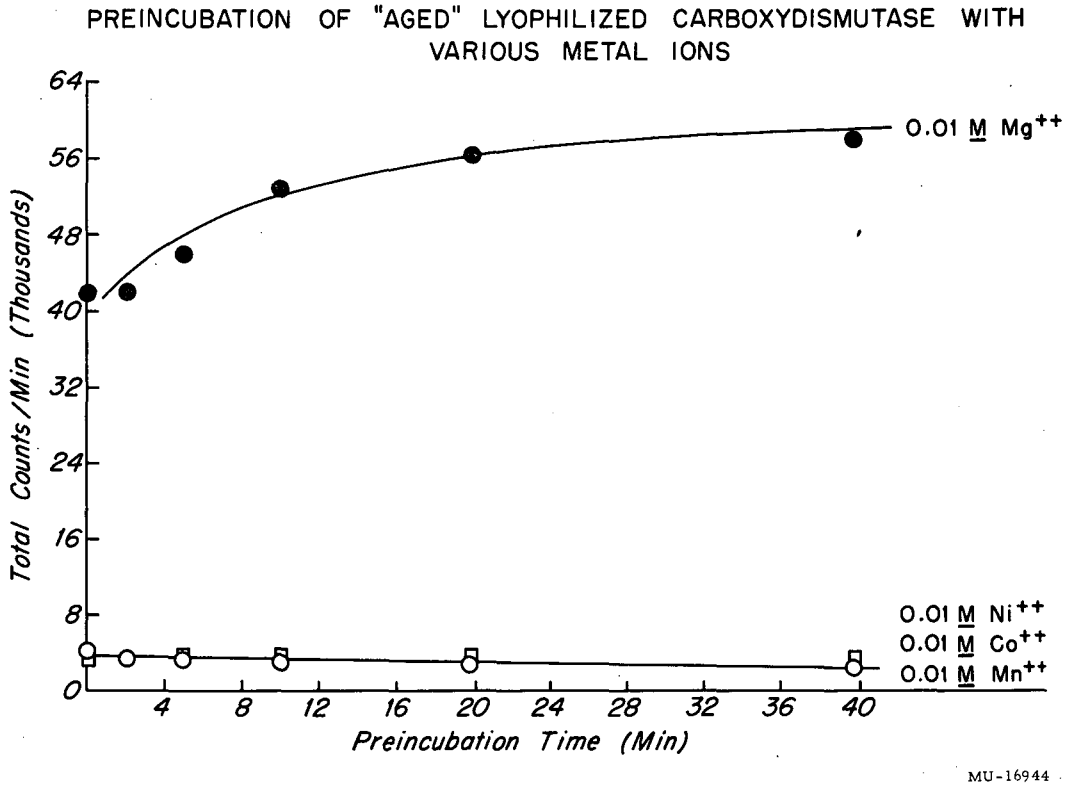

Fig. 19. Preincubation of carboxydismutase with various metal ions.

Additions: enzyme (25μg) plus tris (15μM, pH 8.4); metal ion (all chlorides); $HC^{14}O_3^-$ (1.3 μM, 20μC) plus RuDP (~0.09 μM).

Final volume: made up to 200 μl with distilled water

Conditions: Preincubation temp., 0°C; incubation temp., 25°C; incubation time, 5 min.

In previous experiments, it was concluded that Cr^{+++} is also an activator of carboxydismutase. Actually, this conclusion is erroneous because the activity of the enzyme was based on a measure of the amount of acid-stable fixation product of $C^{14}O_2$; namely, labeled phosphoglyceric acid. Studies with suitable controls--for example, a mixture of Cr^{+++}, labeled bicarbonate and tris--yielded on acid-stable $C^{14}O_2$ fixation product having a composition of one CO_2 molecule to each molecule of Cr^{+++}. The product is probably a carbonato-amine-metal complex.[6]

Preincubation of the enzyme with the substrates yielded the results shown in Figs. 20 and 21. It is quite clear that both Mg^{++} and bicarbonate must combine with carboxydismutase prior to the conversion of RuDP to phosphoglyceric acid. Whether the metal ion complexes with the enzyme before the bicarbonate or vice versa is uncertain.

Another factor to be considered is the fact that in the incubation mixture (pH 8.3) some unlabeled bicarbonate is present. (The amount of unlabeled bicarbonate in all the constituents of the carboxydismutase system excluding the added radioactive bicarbonate was found to be 0.09 μmole. This value is about 7% that of the added labeled bicarbonate.) The unlabeled bicarbonate may, in fact, be bound to the enzyme. According to this view, then, the preincubation effect of the enzyme with bicarbonate is one of exchange or displacement of the bound unlabeled bicarbonate by radioactive bicarbonate.

In summary, the preliminary incubation of carboxydismutase with metal ions and its substrates was investigated. The data are consistent with the idea that Mg^{++} is the "true" cofactor and that an enzyme complexed with both Mg^{++} and bicarbonate must be formed prior to the carboxylation of RuDP.

[6] Arthur E. Martell and Melvin Calvin, Chemistry of the Metal Chelate Compounds, (Prentice-Hall, Inc., New York, 1952), p. 317.

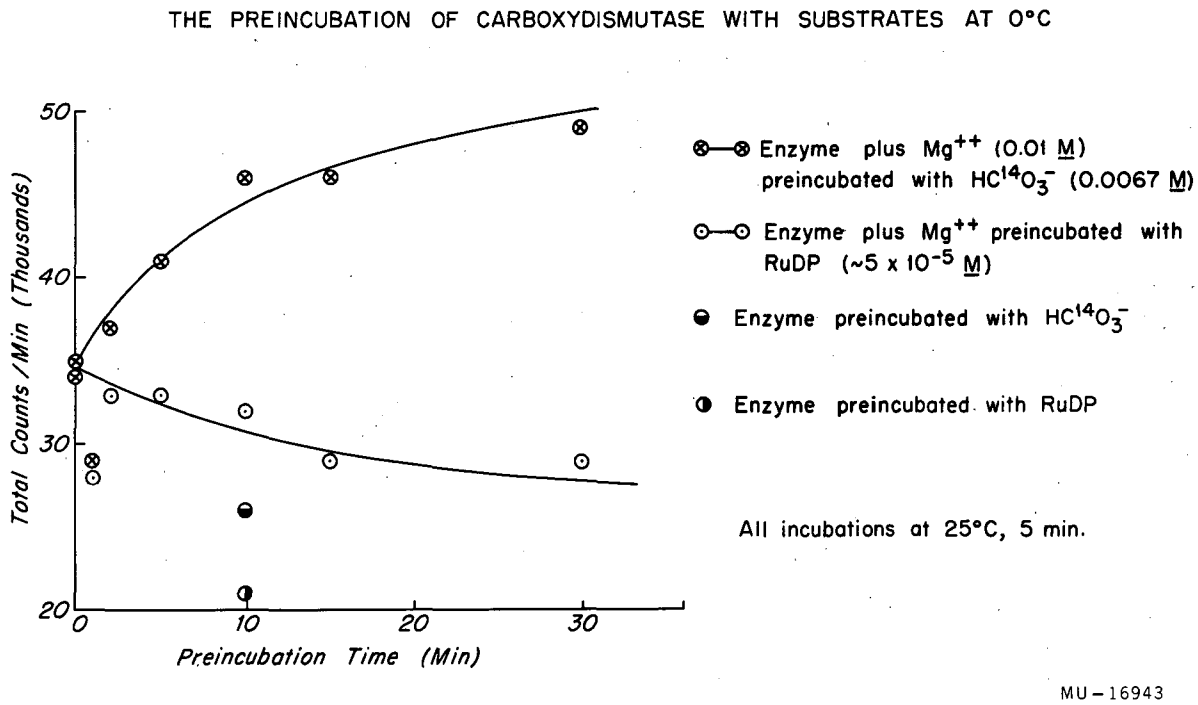

Fig. 20. The preincubation of carboxydismutase with the substrates.

Additions: For ⊗, ⊙: Enzyme (25μg[a]) plus Mg^{++} (2μM MgClz) in tris (15μM, pH 8.3); H_2O to add up to 200 μl final volume; $HC^{14}O_3^-$ (1.3 μM, 20μC) or RuDP (~0.09 μM).

For ◒, ◑: Enzyme, alone (amounts same as above); then substrate; then other substrate plus Mg^{++}.

[a]Enzyme was preincubated with Mg^{++} for 1 min at 25°C, then cooled to 0°C. Rest of conditions are indicated on the graph.

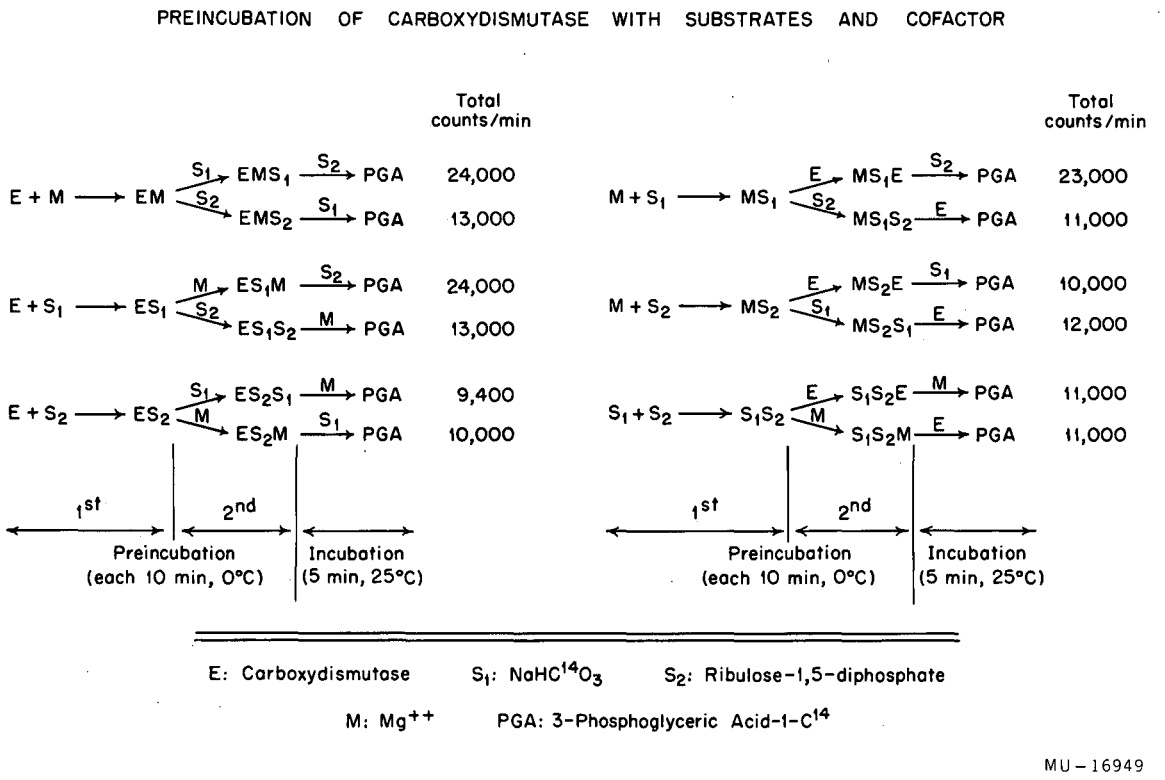

Fig. 21. Preincubation of carboxydismutase with substrates and Mg^{++}.

BIOSYNTHESIS OF MORPHINE ALKALOIDS

Frank R. Stermitz and Henry Rapoport

A number of attempts have been made in this laboratory[1] and elsewhere[2,3,4] to prepare radioactive morphine of high specific activity by growing plants of the opium poppy, Papaver somniferum, in an stmosphere containing $C^{14}O_2$. Growing periods of 21 to 36 days or longer were used, together with total radioactivities of 1 to 2 millicuries of $C^{14}O_2$. The radioactive carbon dioxide was generally given to the plants over the entire growth period. Thus, Kuzin and Merenova,[3] from 20 plants, obtained 260 mg of morphine having an activity of approximately 0.027 μC/mg. Mika,[4] in continuing work of McIntosh, Kelsey, and Geiling,[2] reported obtaining morphine having a specific activity of about 0.36 μC/mg. None of the workers reported any chemical degradation of the morphine obtained to determine the amount of radioactivity present at various positions in the molecule. For our purposes it was necessary to obtain morphine having a high activity in the main carbon skeleton rather than in the relatively much more labile N-methyl group.

Earlier studies here[5,6] have indicated that an increase in alkaloid specific activity might be attained through the use of higher levels of $C^{14}O_2$ activity given over shorter periods of time.

Eight plants of P. somniferum of Afghanistan origin (USDA No. M92) which were 4-1/2 months old and had reached the budding stage were given a total of 24.5 mC of $C^{14}O_2$ in the chamber described previously.[1] In 3 hours, 70% of the activity had been absorbed, and more than 90% was absorbed in the first 24 hours. After 44 hours, approximately 7.3 mC of $C^{14}O_2$ was introduced into the chamber, followed by 4.1 m at 116 hours and about 1 mC at 140 hours. Nonradioactive carbon dioxide was added at 146 hours, and the plants were killed at the end of 166 hours. During the course of the experiment, carbon dioxide concentration in the chamber varied from about 0.02% to 0.3%. The radioactivity in the chamber was generally from 0.4 to 1.0 mC except for a few hours after each introduction of $C^{14}O_2$, when the higher levels noted were reached. Since the chamber was closed, carbon dioxide concentration and activity were higher at the end of the daily dark period, owing to plant respiration. The plants were maintained on a 15-hour day with artificial light giving approximately 1000 foot-candles in the chamber.

---

[1] Henry Rapoport, Don R. Baker, and Melvin Look, in Chemistry Division Quarterly Report, UCRL-8204, March 1958, p. 21.

[2] B. J. McIntosh, F. E. Kelsey, and E. M. K. Geiling, J. Am. Pharm. Assoc. 39, 512 (1950).

[3] A. M. Kuzin and V. I. Merenova, Biokhimiya 19, 616 (1954).

[4] E. S. Mika, Botan. Gaz. 116, 323 (1955).

[5] Don R. Baker, Ph. D. Thesis, University of California, Berkeley, California, 1959.

[6] Henry Rapoport and Frank Stermitz, in Chemistry Division Quarterly Report, UCRL-8575, Dec. 1958, p. 32.

At the end of 166 hours, the plants were cut in small pieces into liquid nitrogen and were ground to a powder. The wet weight was 170 grams. The powder was extracted for 20 hours in a Soxhlet extractor with 95% ethanol. Further work-up was according to the procedure of Baker,[1] with the exceptions that chloroform was used in place of methylene chloride in the morphine extraction at pH 8.6 and that an additional extraction procedure was used in place of cellulose-powder-column chromatography for the final morphine purification.

A total of 37.1 mg of morphine having a specific activity of 3.62×10^6 dpm/mg (1.03×10^6 dpm/μmole) was isolated. As had been previously observed,[6] this procedure yielded only traces of thebaine. A portion of the morphine was degraded to normorphine by the Von Braun procedure, and the resulting demethylated compound had a specific activity of 2.52×10^6 dpm/mg (6.90×10^5 dpm/ μmole). Thus, 67% of the activity of the original morphine is located in the nucleus, and a demethylation and remethylation procedure[7] would result in morphine having an activity of 1.12 μC/mg.

In a second experiment, four plants of P. somniferum (USDA No. 40, a variety of lower alkaloid content than No. M92) which were 3-1/2 months old and at the budding stage were used. They were given 23.5 mC of $C^{14}O_2$ in the chamber and then grown for 8 days. This time, only nonradioactive carbon dioxide was used to maintain the level in the chamber throughout the period. The plants were killed in the same manner and the wet weight was 190 g.

Leete's modification[8] of the procedure of Achor and Geiling[9] was used to isolate the alkaloids. A total of 48 mg of morphine, together with 5.2 mg of codeine and 3.4 mg of thebaine was isolated. The following specific activities were observed;

Compound	10^6dpm/mg	10^6dpm/μmole
morphine	1.57	0.448
codeine	1.98	0.592
thebaine	2.24	0.696

A portion of the morphine was diluted and converted to normorphine. It was found that 92.5% of the activity of the original morphine was present in the main carbon skeleton.

---

[7] M. Look and H. Rapoport, in Chemistry Division Quarterly Report, UCRL-3629, Jan. 1957, p. 37.

[8] E. Leete, J. Am. Chem. Soc., in press (1959).

[9] L. B. Achor and E. M. K. Geiling, Anal. Chem. 26, 1061 (1954).

Thus, it appears that, for producing morphine with a strictly skeletal label, maintaining an appreciable amount of $C^{14}O_2$ in the chamber over the entire growth period has no advantage over using the same amount of activity in one large dose at the beginning of the biosynthetic period. One further experiment is now being conducted in which four of the USDA No. 40 poppies were given a total of 39.2 mC of $C^{14}O_2$ at one time. The preliminary results of this study indicate that this is indeed the best method for obtaining morphine labeled in the manner desired.

The alkaloids isolated from the first two experiments will now be used for chemical degradations which may indicate some of the modes of entrance of carbon into the alkaloid molecule. The biosynthetic experiment now being conducted will provide labeled morphine for use in human and possibly plant metabolism studies.

ADENINE METABOLISM IN MICE MAINTAINED ON DEUTERIUM OXIDE

Edward L. Bennett and Nancy Dye

Results of previous investigations of the effects of deuterium oxide on biological systems (e.g., Chlorella,[1] mouse ascites tumors,[2] mouse sperm,[3] and cells in tissue culture) have suggested that the process of cell division may be inhibited by D_2O. Changes in the rate of cell division have frequently been measured by comparison of the rate of incorporation of nucleic acid precursors such as phosphate, glycine, and adenine into ribonucleic acid (RNA) and deoxyribonucleic acid (DNA) of control and experimental animals.

We have continuously administered 30% D_2O in drinking water to C57 male mice for an extended period of time. We have studied the effect of this treatment on the incorporation of adenine into the soluble nucleotide 5'-adenylic acid derivatives, RNA adenine and guanine, and DNA adenine and guanine. These compounds were isolated from the spleen, thymus, small intestine, large intestine, and carcass(including bone marrow) at 24 hours after adenine-C^{14} injection.

Two experiments have been performed. In each, three experimental and three control mice were used. In the first experiment, the experimental mice were 2 months old when they were first given 30% D_2O in the drinking water, and they were maintained on this water for 3 months. In the second experiment, the mice had been maintained on 30% D_2O for 5 months. The experimental and control mice in each experiment were littermates, and matched in body weight within 1 g. Each mouse was administered intraperitoneally 1.2 mg of adenine-8C^{14} (10μC) and sacrificed 24 hours later. Corresponding tissues from the respective mice were pooled and the nucleotides and nucleic acid fractions were isolated and analyzed as previously described.[4]

The specific activities obtained for each fraction are summarized in Table VI. In addition, the ratio of the specific activity in the experimental animal to that in the control is calculated for each tissue and fraction. It appears that, with the possible exception of the carcass, there was very little difference in incorporation of adenine into the 5'-adenylic acid fraction of the soluble nucleotide pool, although the specific activity found at 24 hours in the soluble-nucleotide fraction of the experimental animals was slightly less than in the control in each comparison.

---

[1] V. Moses, O. Holm-Hansen, and M. Calvin, Biochim. Biophys. Acta, 28, 62 (1958).

[2] A. Hughes, B. Tolbert, K. Lonberg-Holm, and M. Calvin, Biochim. Biophys. Acta, 28, 58 (1958).

[3] A. Hughes, E. L. Bennett, and M. Calvin, Proc. Nat'l. Acad. Sci. U.S., 45, 581 (1959).

[4] E. L. Bennett and H. Karlsson, J. Biol. Chem. 229, 39 (1957).

TABLE VI

COMPARISON OF SPECIFIC ACTIVITY OF NUCLEOTIDES AND NUCLEIC ACID PURINES OF NORMAL MICE AND MICE MAINTAINED ON 30% D_2O AFTER INJECTION OF ADENINE-C^{14}

Tissue		5-AMP		RNA				DNA			
				Adenine		Guanine		Adenine		Guanine	
		Exp. 1	Exp. 2	Exp. 1	Exp. 2	Exp. 1	Exp. 2	Exp. 1	Exp. 2	Exp. 1	Exp. 2
Spleen	Control		808	407	405	59	79	68	73	14	15
	Exp		715	370	363	74	91	91	109	28	34
	Ratio E/C		0.88	0.91	0.90	1.25	1.15	1.34	1.49	2.00	2.26
Thymus	Control	--	6.27	426	268	26?	57	148	175	8.3	13
	Exp.	--	553	324	228	29	43	116	134	13	17
	Ratio E/C		0.88	0.76	0.85	1.12?	0.75	0.78	0.77	1.57	1.31
Sm.Int.	Control	1331	1491	553	584	67	89	286	257	56	48
	Exp	1144	1467	559	562	107	101	287	234	66	60
	Ratio E/C	0.86	0.98	1.01	0.96	1.60	1.14	1.00	0.91	1.18	1.25
Lg.Int.	Control	1110	1151	716	711	133	161	246	279	42	49
	Exp.	1008	1137	624	635	137	205	194	260	47	59
	Ratio E/C	0.91	0.98	0.87	0.89	1.03	1.27	0.79	0.93	1.12	1.20
Carcass	Control	218	217	168	174	34	23	145	149	31	35
	Exp	160	174	178	187	44	40	148	138	45	44
	Ratio E/C	0.73	0.80	1.06	1.07	1.29	1.74	1.02	0.93	1.45	1.26

The effect of D_2O upon the incorporation of adenine into the nucleic acids is apparently complex. However, it appears that the conversion of adenine into guanine and incorporation into nucleic acid is enhanced, particularly in the DNA fraction. The effect seems to be more pronounced in the spleen than in the other tissues investigated. The incorporation of adenine into nucleic acid adenine does not appear to be significantly affected except possibly in the DNA in spleen. In this tissue, the increased incorporation may be an indication of increased cell renewal due to the stress of D_2O administration. In the thymus, adenine incorporation into nucleic acid adenine may be slightly depressed.

At present one can speculate that D_2O may interfere with the biosynthesis of guanine, and that thus more adenine, when available, is converted to guanine by known biosynthetic routes. Except possibly in the spleen, it does not appear that chronic D_2O administration markedly influences the renewal rate of the nucleic acids in the mouse.

PROTEIN CONTENT OF RAT BRAIN: STRAIN AND AREA DIFFERENCES

Edward L. Bennett, Ann Ohlander, and Hiromi Morimoto

(In collaboration with Professor David Krech and Mark R. Rosenzweig, Psychology Department, University of California, Berkeley)

In our previous work we have concerned ourselves primarily with the relation of rat-brain cholinesterase to behavior.[1] Inasmuch as cholinesterase is a protein, the question can be raised whether our observations merely reflect the relationship between brain protein and behavior rather than, more specifically, between cholinesterase and behavoir. For this reason a protein analysis has been made of animals from four strains known to have differences in cholinesterase levels.

Protein content was determined with the Folin phenol reagent as described by Lowry et al.[2] Duplicate aliquots of the saline homogenates of the rat cortex or subcortical brain containing 1 mg wet weight of tissue were mixed with 5 ml of Reagent C in 12-ml tubes. After 10 minutes 0.50 ml of the diluted Folin-Ciocalteau phenol reagent was added and rapidly mixed. The optical density at 750 mμ was determined in 1-cm cells in a Beckman DU spectrophotometer after 45 minutes. Suitable aliquots of a freshly diluted crystalline bovine albumin solution (Armour) were run with each series as standards, and all results have been referred to this standard (% protein = % N x 6.25). The absolute amount of protein may be slightly different from the values reported, as the color intensity for different proteins may not be the same as that obtained from the standard albumin. In addition, a small proportion (<5%) of the color is probably due to nonproteinaceous material.[2] However, within the rat cortex and brain, deviations from the correct absolute value are undoubtedly small, and relative differences found are significant.

Table VII presents the data for 72 S_1 rats divided among six age groups (ranging in age from 13 days to 465 days). The table gives the percent of protein in the brain for the visual (v) cortex, somesthetic (s) cortex, and subcortical tissue. ("Subcortex" is used here to mean the total brain minus the dorsal cortex, which has been removed.) Also presented are the standard deviations (SD) for each measurement. It will be seen that the values increase with age for each measurement, reaching a plateau at about 100 days of age. The change of protein content with age is quite similar to one presented by Folch-Pi[3] for whole brain of the mouse.

---

[1] Edward L. Bennett, Hilda Roderick, Ann Ohlander, Thomas H. Roderick, Hiromi Morimoto, and Charles Longueil, in Chemistry Division Quarterly Report, UCRL-8575, Dec. 1958, p. 34.

[2] O. H. Lowry, N. J. Rosebrough, A. L. Farr, and R. J. Randall, J. Biol. Chem. 193, 265 (1951).

[3] J. Folch-Pi, in Biochemistry of the Developing Nervous System, H. Waelsch, Ed., Academic Press, New York, New York, 1955.

TABLE VII

PERCENT PROTEIN, S_1 STRAIN

Age	No. of Animals	Visual Cortex % Protein	SD	Somesthetic Cortex % Protein	SD	$\frac{V+S}{2}$	SD	Sub-cortex % Protein	SD
13	15	7.0	.47	7.1	.59	7.1	.48	7.6	.14
21	14	8.8	.27	8.5	.75	8.6	.44	9.1	.08
61	14	10.4	.22	10.1	.38	10.3	.23	10.2	.15
105	9	10.9	.16	11.0	.24	11.0	.17	10.7	.20
353	9	11.2	.18	10.9	.33	11.0	.24	10.6	.20
465	11	10.9	.30	11.1	.31	11.0	.28	10.5	.12

$\frac{V+S}{2}$ = Average protein content of visual and somesthetic cortex

SD = Standard deviation

The growth function observed in Table VII is congruent with the data presented in Table VIII (percent protein for 26 S_3 rats of three different ages). One interesting aspect of this growth curve is presented in Table IX, which indicates quite unambiguously that at the early ages (less than 60 days) the percentage of protein in the subcortex is greater than that in the cortex; at approximately 50 days the lines cross and the percentage of protein is greater in the cortex than in the subcortex. This is clearly shown in Figure 22. A similar analysis for the S_3 rats (Table X) indicates that the same thing appears for this strain, with the suggestion that the crossover may occur at a somewhat later age. The data of Tables VII and VIII also indicate clearly that there is no difference in percent of protein between the visual and somesthetic areas (unlike, of course, the situation with cholinesterase). Also, the difference between cortical and subcortical protein is rather small, while the subcortex contains 2.5 times as much cholinesterase per unit weight as the cortex contains. Scatter plots for the S_1 and S_3 rats indicate no relationship between protein and cholinesterase.

The relative variability of the percent-protein determination can be expressed by the coefficient of variation: $\frac{SD}{\bar{X}} \times 100$. For analyses of the S_1 and S_3 strains more than 60 days in age, the coefficient of variations is approximately 2.0 for the cortex and 1.4 for the subcortex. For animals less than 60 days of age, the coefficient for the cortex is approximately 6.0, while that for the subcortex is again about 1.4. These variabilities are considerably less than the variabilities we have found for cholinesterase, which are of the order of 5.0. The variability of cholinesterase is higher than the variabilities we have previously found for lactic dehydrogenase and for brain weight. Thus, of the four types of analyses we have thus far made, cholinesterase shows the greatest individual variability. This is encouraging since it suggests that the level of this enzyme could exhibit a higher degree of relationship to individual differences in behavior than any of the other biochemical variabilities thus far investigated.

In summary: First, although previous experiments have shown that these two strains of rats differ significantly in cholinesterase and in behavior, the present data indicate that the strains do not differ with respect to percentage of protein. Secondly, the change of protein content with age of animal is quite different from the change of cholinesterase activity with age of animal. Thirdly, where cholinesterase shows significant and consistent differences in activity per unit weight of tissue from one functional area of the cortex to the other (visual and somesthetic), the protein percentage fails to show any difference. Fourthly, the cortex of animals more than 60 days of age is slightly higher in percentage of protein than the subcortex, but it is much lower in cholinesterase activity. Finally, percentage of protein shows very low variability among individuals.

The data on the RDH and RDL strains of rats are fragmentary. Table XI presents these data, and --as can be seen--we have 15 animals age 102 days of the RDH strain and 18 animals age 96 days of the RDL strain. We are at present analyzing more animals of these two strains. On the basis of the available data, the following tentative conclusions may

TABLE VIII

PERCENT PROTEIN, S_1 STRAIN

	Age	No. of Animals	Visual Cortex % Protein	SD	Somesthetic Cortex % Protein	SD	$\frac{V+S}{2}$	SD	Sub-cortex % Protein	SD
	103	9	10.9	.10	10.6	.27	10.7	.16	10.9	.10
$\frac{SD}{\bar{X}} \times 100$				0.9		2.5		1.5		0.9
	368	8	11.2	.20	10.9	.22	11.0	.14	10.6	.15
$\frac{SD}{\bar{X}} \times 100$				1.8		2.0		1.3		1.4
	467	9	10.9	.24	11.1	.26	11.0	.20	10.5	.10
$\frac{SD}{\bar{X}} \times 100$				2.2		2.3		1.8		1.0

$\frac{V+S}{2}$ = Average protein content of visual and somesthetic cortex

SD = Standard deviation

TABLE IX

RELATION BETWEEN CORTICAL AND SUBCORTICAL PERCENT PROTEIN, S_1

Age	13	21	61	105	353	460
	No. of Comparisons					
Cor ≤ Sub	15	14	10	3	1	1
Cor > Sub	0	0	4	6	8	10
% Cor ≤ Sub / Total	100	100	71	33	11	9
$\bar{X}$ diff	.57	.47	-.03	-.27	-.46	-.52

$\bar{X}$ diff = Average percentage of protein in subcortex minus average percentage of protein in visual and somesthetic areas of cortex.

TABLE X

RELATION BETWEEN CORTICAL AND SUBCORTICAL PERCENTAGE PROTEIN, S_3

Age	103	368	460
	No. of Comparisons		
Cor < Sub	7	0	0
Cor > Sub	2	8	9
% Cor ≤ S / total	78	0	0
$\bar{X}$ diff	.20	-.47	-.50

$\bar{X}$ diff = Average percentage of protein in subcortex minus average percentage of protein in visual and somesthetic areas of cortex.

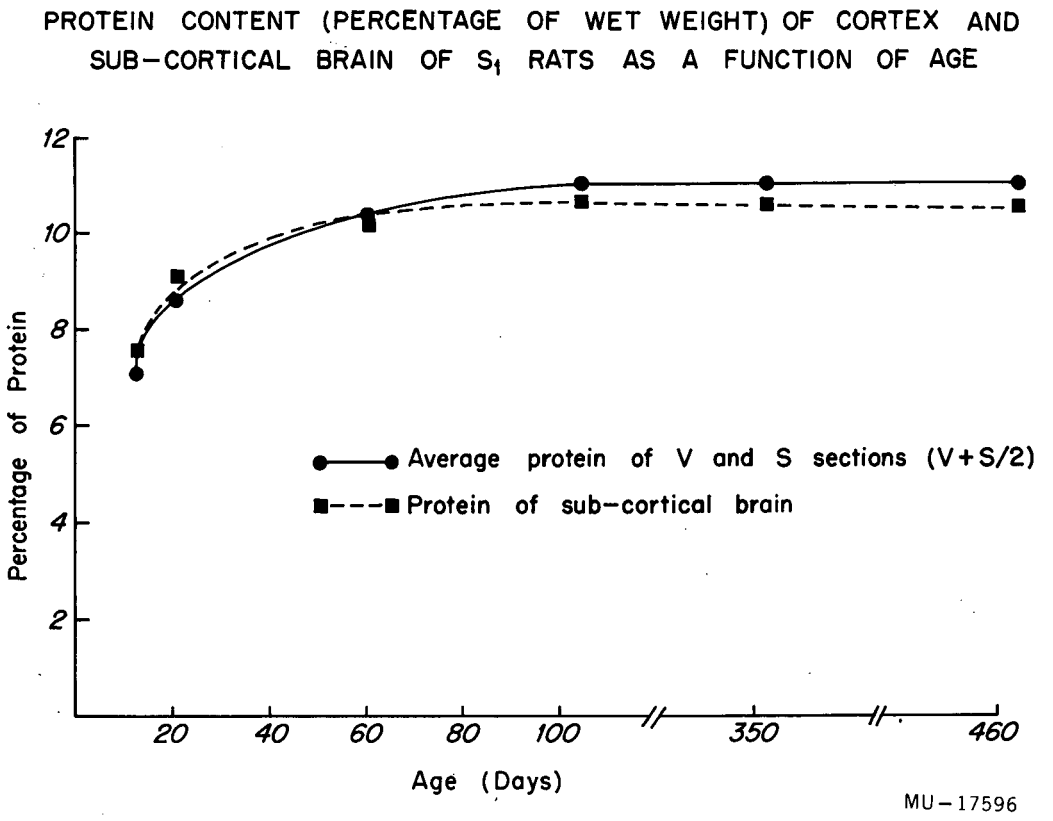

Fig. 22. Protein Content in % of wet weight of cortex and Sub-cortical brain of S_1 rats as a function of age.

TABLE XI

PERCENT PROTEIN, RD STRAINS

Strain	Age	No. of Animals	Visual Cortex	SD	Somes-thetic Cortex	SD	$\frac{V+S}{2}$	SD	Sub-Cortex	SD
RDH	102	15	11.4	.68	12.3	.93	11.9	.67	10.1	.33
RDL	96	18	11.4	.57	12.2	.67	11.8	.54	10.1	.31

$\frac{V+S}{2}$ = Average protein content of visual and somesthetic cortex

SD = Standard deviation

be suggested: First, although these two strains differ by about 25% in cortical cholinesterase, their percentages of cortical protein are identical. For these strains there appears to be a significant difference between the two cortical areas, the S area having a higher percentage of protein than the V area. As in the S_1 strain, the cortical-protein value is significantly higher than the subcortical value at about 100 days of age. For these two strains the coefficients of variation in percentage of protein are apparently the same as the coefficients of variation in cholinesterase -- about 5%. Here, as in the S_1 and S_3 strains, the variability is lower in the subcortical measurements than in the cortical measurements, perhaps because the analysis was based on a considerably larger amount of tissue. Finally, it appears that the RDH and RDL strains have significantly higher cortical percentages of protein than the S_1 and S_3 strains, but the RDH and RDL strains have significantly lower subcortical protein than the S_1 and S_3 strains.

Over-all tentative conclusions: Percent of protein does not seem to be correlated with cholinesterase activity. It therefore appears highly unlikely that our observed correlations between cholinesterase and behavior reflect only an underlying relationship between over-all protein and behavior.

EFFECT OF CRYSTAL SIZE ON THE RADIATION SENSITIVITY OF CHOLINE CHLORIDE

Richard M. Lemmon and Bernice Soltysik

In our continuing studies of the mechanism of the radiation decomposition of crystalline choline chloride,[1] it has been of interest to inquire into the mechanism by which the free-radical chain finally comes to a halt. It is reasonable to suppose that a radical-propagating chain might end as soon as the chain reached the surface of a crystal. We therefore decided to test the influence of crystal size upon choline chloride's radiation sensitivity.

Large and small crystals of choline chloride were grown in the following manner: Large crystals were obtained by allowing a concentrated ethanol solution to cool very slowly. A large crystal was broken into a few pieces which were fitted into glass tubes (4 mm i.d.) for irradiation. Small crystals were obtained by rapidly precipitating choline chloride as a fine powder from an ethanol solution by pouring the solution into three volumes of chilled, stirred ether.

Two tubes each (evacuated and sealed) of the large and small crystals were simultaneously irradiated for 15 minutes in a Co^{60} γ-ray source. The crystals were irradiated in equivalent positions and they received a total of 1.7×10^6 rads of the γ radiation. The extent of decomposition was measured by the total amount of volatile amine (predominantly, if not entirely, trimethylamine) that appeared as a result of the irradiation.[1] For each sample irradiated, a blank determination was carried out on similar but unirradiated crystal. In all cases, the blanks were essentially zero, i.e., no volatile amines or amine salts were present prior to irradiation. The results, shown in Table XII, indicate that a higher percentage of radiation decomposition occurs in the finer crystals.

It is possible that the fine crystals that were used in the above work occluded higher percentages of impurities than did the large crystals. Consequently, the amounts of surface area in the two sizes of crystals may not have been the only variable. We therefore decided to repeat the same experiment using, on the one hand, the same large crystals and, on the other hand, very small crystals obtained by grinding some of the large crystals to a fine powder. The experiment was also repeated on another sample of fine crystals obtained from rapid crystallization. The results are also shown in Table XII. It is apparent that the small crystals, whether obtained by rapid crystallization or by grinding, show a higher percentage of decomposition than do large crystals.

The results of these experiments clearly indicate that the propagation of free-radical chains does not cease at crystal surfaces; if they did, the amounts of decomposition would be less, not more, in the smaller crystals. It seems strange that the two types of small crystals (those rapidly crystallized and those obtained by grinding a large crystal) exhibit the same decomposition percentages since undoubtedly the average sizes were different in the two types. However, as an explanation of the different decomposition percentages between large and small crystals, one can

[1] R. O. Lindblom and R. M. Lemmon, in Bio-Organic Chemistry Quarterly Report, UCRL-8575, Dec. 1958, p. 11.

suppose that the greater concentration of electron traps at defects in the small crystals leads to greater free-radical stability, and thus to more decomposition.

Table XII

Decomposition of large and small irradiated choline chloride crystals (in percent) (Dose: 1.7×10^6 rads)

	Experiment 1	Experiment 2
Small crystals	15.9	15.1
	15.7	--
Large crystals	11.7	11.6
	12.7	11.5
Finely ground crystals	--	15.5
(from large crystals)	--	15.1

THE CHEMISTRY OF N-CARBOXY-L-GLUTAMIC ACID ANHYDRIDE: A PRELIMINARY REPORT

Yoshiro Ogata

There are many reports on the preparation and properties of esters of N-carboxyglutamic acid anhydride (I).[1,2] However, we have only one report on N-carboxyglutamic acid anhydride (CAGA) itself (II). Stahman and co-workers[3] reported that N-carboxyglutamic acid anhydride

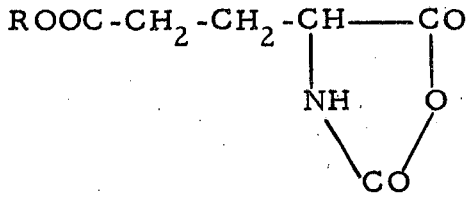

(I)

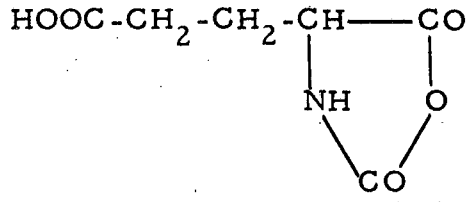

(II) (CAGA)

can be prepared by the catalytic hydrogenation of the benzyl ester of N-carboxyglutamic acid anhydride and that the CAGA obtained gives a polymer in aqueous solution. No description of the experimental details was given in this report.

In connection with the possible role of glutamic acid in carboxylation in the photosynthetic cycle, we were interested in investigating preparation and properties of N-carboxy-L-glutamic acid anhydride (CALGA). The following data summarize the results we obtained on the chemical properties of CALGA.

Experimental Procedure

Preparation of γ-benzyl-N-carboxy-L-glutamate anhydride

γ-Benzylglutamate was prepared by the hydroiodic-acid-catalyzed esterification of glutamic acid with benzyl alcohol according to the method of Hanby, Waley, and Watson.[4] Upon recrystallization from water, colorless plates were obtained, m.p. 173-174° (lit.[4] 170°).

Finely powdered γ-benzyl glutamate (15 g) was suspended in 300 ml of dioxane, and phosgene was introduced at 45° for about 80 minutes. A magnetic stirrer was used . The phosgene addition was then stopped and the solution was stirred at the same temperature for 1 hour until a clear solution was obtained. The solvent was distilled off in vacuum on a water bath maintained at 45-50°. The residual crystals were dissolved in 125 ml of ethyl acetate, activated charcoal was added, and the solution was filtered. Petroleum ether (about 300 ml) was added to the filtrate to precipitate the product. The product was washed with petroleum ether and dried.

[1] C. H. Bamford, A. Elliott and W. E. Hanby, Synthetic Polypeptide Preparation, Structure and Properties, Academic Press, New York, N. Y. (1956).

[2] E. Katcholski and M. Sela in Adv. in Protein Chem., 12, 243 (1958).

[3] M. A. Stahman, H. Tsuguki and H. J. Van Kley, Congr. intern. biochem. Resumes communs. 3e Congr. Brussels, 1955, 13. Cf. C.A., 50, 14203 (1956).

[4] W. E. Hanby, S. G. Waley and J. Watson, J. Chem. Soc., 1950, 3239.

The yield was 13.2 g (78%), m.p. 93-94° (lit.[4] 97°).[5]

Anal. Calc'd for $C_{13}H_{13}O_5N$: C, 59.31; H, 4.98[2]; N, 5.32

Found: C, 58.95; H, 5.11; N, 5.40.

Preparation of N-carboxy-l-glutamic acid anhydride.

The benzyl ester obtained above (1 g), 0.5 g of palladium charcoal catalyst, and 10 ml of dioxane were placed in a pressure flask and the flask was shaken under 3 atmos initial hydrogen pressure at room temperature (21-24°) for 40 minutes. The pressure drop observed was in accordance with the theoretical value. After filtration, the solution contained a small amount of toluene that originated from the benzyl group. Owing to decomposition, the solution became turbid on standing at room temperature. Even when the solution was kept in a refrigerator at -30°, about one-half the CALGA was decomposed within 3 days.

The weight of the dioxane solution obtained above was measured and an aliquot (0.2 ml) was taken and diluted to 10 ml with distilled water. The aqueous solution obtained was titrated with 0.01 N sodium hydroxide. The resulting product showed that the yield of the acid obtained by hydrogenation was quantitative, i.e., 98-100%. However, the acid was too unstable to isolate. Even if benzene was added to the solution and vacuum-evaporated, after vacuum evaporation of the dioxane, followed by repetition of the same procedure, the solvent was still occluded in the product. Therefore the acidimetry of the product gave variable and inconsistent molecular-weight and analysis data. For example:

Anal. Calc'd for $C_6H_7O_5N$: Mol. wt., 173.12; found, 187.

Calc'd: C, 41.62; H, 4.08[2]; N, 8.09

Found: C, 45.08[2]; H, 5.27; N, 6.36

The residue obtained by evaporation of dioxane alone seems to contain about 1 mole of dioxane per mole of the acid.

Anal. Calc'd for ($C_6H_7O_5N + C_4H_8O_2$) Mol. wt., 261; found, 268.

Calc'd: C, 45.97; H, 5.79; N, 5.36

Found: C, 44.6; H, 5.3; N, 5.9 (volatile--difficult to obtain accurate values)

The solvent seems necessary for the stability of the acid.

---

[5] The m.p. could not be raised to the value given in the literature upon recrystallization.

When a smaller amount of the catalyst was used in the hydrogenation, the reaction took a longer time. If the amount of catalyst for the usual hydrogenolysis (e.g., 0.1 g/g of ester) was used, the result was quite unsatisfactory, since the product (a white powder) was the polymer of the starting material. The analysis of the polymer showed that it was the polypeptide of benzylglutamate, melting at above 200°.

Anal. Calc'd for $(C_{12}H_{13}O_3N)_n$: C, 65.74; H, 5.98; N, 6.39.

Found: C, 65.52; H, 5.93; N, 6.31

The same polymer was more easily obtained upon hydrogenation with platinum oxide.

Properties of CALGA in dioxane solution

When the dioxane solution of CALGA was evaporated with a rotating vacuum evaporator at room temperature, a colorless gel was obtained which contains about 1 mole of dioxane per mole of CALGA. However, the gel was easily decarboxylated, especially in the presence of moisture, to give crystals of 3, 6-diketopiperazine-2, 5-dipropionic acid (III),[6,7] m.p. 160-161° (lit.[7] 161°).

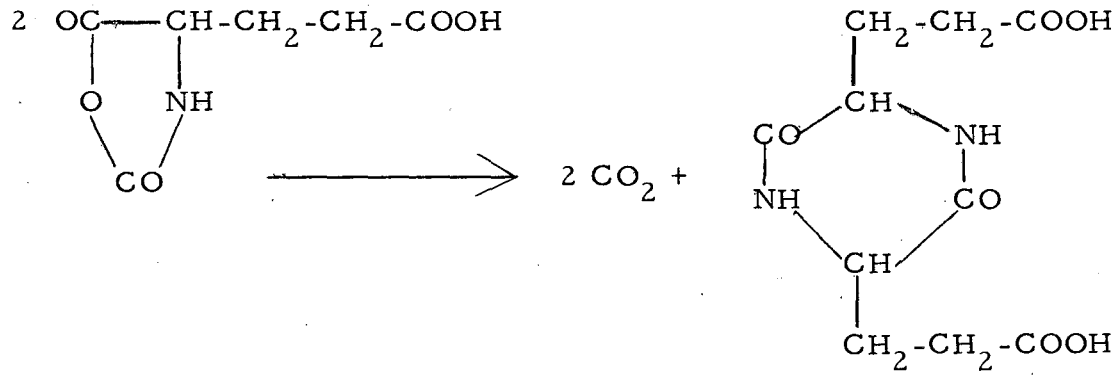

(III)

Anal. Calc'd for $C_{10}H_{14}O_6N_2$: C, 46.51; H, 5.47; N, 10.85.

Found: C, 46.28; H, 5.32; N, 10.59

[6] J. A. King and F. H. McMillan, J. Am. Chem. Soc. 74, 2859 (1952).

[7] A. F. Beecham, J. Am. Chem. Soc. 76, 4613 (1954).

Titration of the acid (III) agreed with theory, i.e., a measured amount of the acid (III) was titrated with 0.01 N sodium hydroxide with phenolphthalein as an indicator; then the molecular weight calculated for $C_{10}H_{14}O_6N_2$ as dibasic acid is 258; found 260.

The CALGA in dioxane solution gave a brown-purple color upon addition of aqueous hydroxylamine and then ferric ammonium sulfate. The absorption maximum of the solution was 474 mμ. The CALGA-dioxane gel is soluble in ethyl acetate and acetone, soluble with difficulty in ethyl ether, and insoluble in benzene, carbon tetrachloride, and petroleum ether.

Kinetic study of the decarboxylation of CALGA

To investigate the behavior of CALGA in aqueous solutions and to study the effect of pH on the rate of decomposition, rate measurements were carried out in aqueous buffers. The reaction of CALGA with water gave pure 3, 6-diketopiperazine-2, 5-dipropionic acid (III), m.p. 161°. There was no indication of high-molecular-weight product, at least under the conditions of the three kinetic runs performed.

a. Experimental procedure

A mixture of 0.5 g of CALGA, 0.25 g of palladium-charcoal, and 5 ml of dioxane was hydrogenated as described above. After filtration, the solution was weighed, and the content of the acid was determined by the acidimetry.[8] One ml of the solution was taken out and diluted to 10 ml with a mixture of dioxane and toluene (8:2 by volume). When the solution was kept at 0° this solvent mixture was necessary to prevent freezing. For the kinetic study above 10°, pure dioxane may be used as the solvent.

An aliquot of 0.2 ml was taken from the dioxane-toluene solution and introduced into the side arm of a Warburg apparatus. Two ml of a buffered solution was introduced into the main flask of the Warburg, the apparatus was connected, and after 20 minutes of shaking in the thermostat to obtain the temperature equilibrium, the two solutions were mixed. The readings were corrected by comparison with a reading of solvents alone.

As shown in Fig. 23 an experiment in which citrate buffers and aqueous sodium bicarbonate was used indicated that the evolution of carbon dioxide reached equilibrium after 10 minutes at 0° in the pH range below 4.95. Unfortunately, the reaction of CALGA was found to be very rapid. Therefore, the estimations were limited to 10-25 minutes from the start of the reaction, giving only an approximate value of the rate.

b. Results

The results with citrate buffers are shown in Table XIII and Figs. 24 and 25, which show the apparent tendency of acceleration of the

[8] The volume of CO_2 evolved in the kinetic runs agreed with that expected from the acidimetry.

The Effect of pH on the Rate of Evolution of CO_2 from $NaHCO_3$ in Aqueous Citrate Buffers at 0°

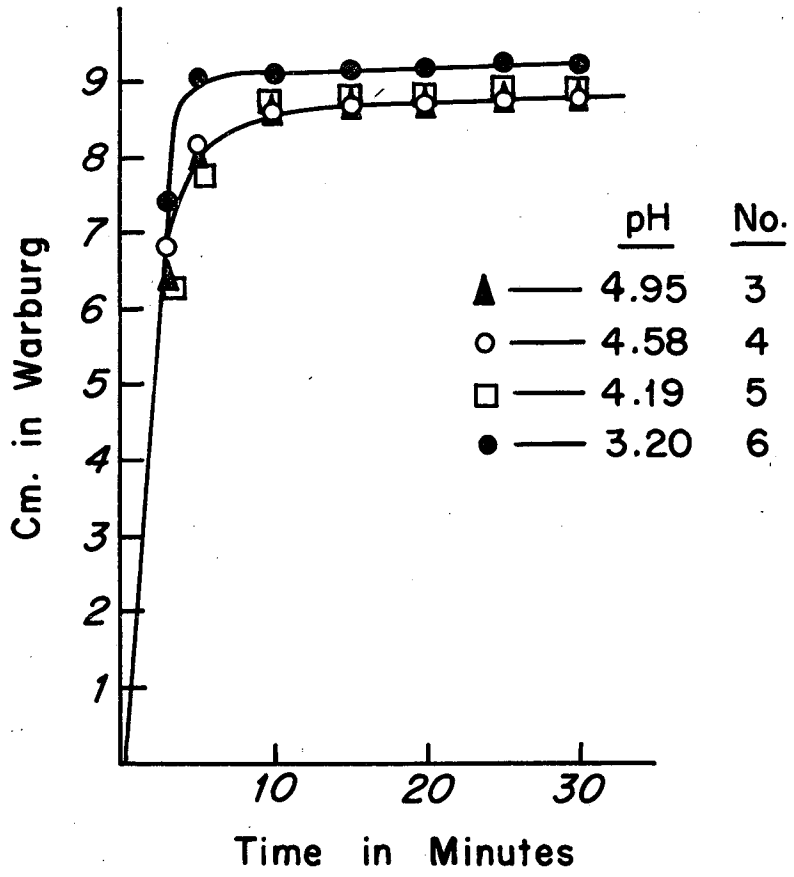

MU-17494

Table XIII

First-order rate constants in citrate buffers[a] ($k \times 10^2$ sec^{-1})

pH[b]:	4.95	4.58	4.19	3.68	3.20
min					
5	1.080	2.58	3.61	3.67	3.88[c]
10	1.880	2.87	3.61	4.97	4.81
15	2.060	2.98	4.07	3.94	5.00
20	2.170	3.08	2.62	3.62	very fast
25	2.270	3.04	2.89	fast	
30	2.446	2.61	2.92		(c)
Ave.	2.145	2.99	3.55	4.17	4.91

[a]The rates were too rapid to estimate at pH below 3.2, and they were unreliable at pH above 5 because of the slow and incomplete evolution of carbon dioxide which was found in the test using sodium bicarbonate.

[b]There was no appreciable change of pH upon addition of the reactant or during the reaction itself.

[c]The data at 5 and 30 minutes were not used in determining the average.

The Effect of pH on the Rate of Evolution of CO_2 from CAIGA in Aqueous Citrate Buffers at 0°

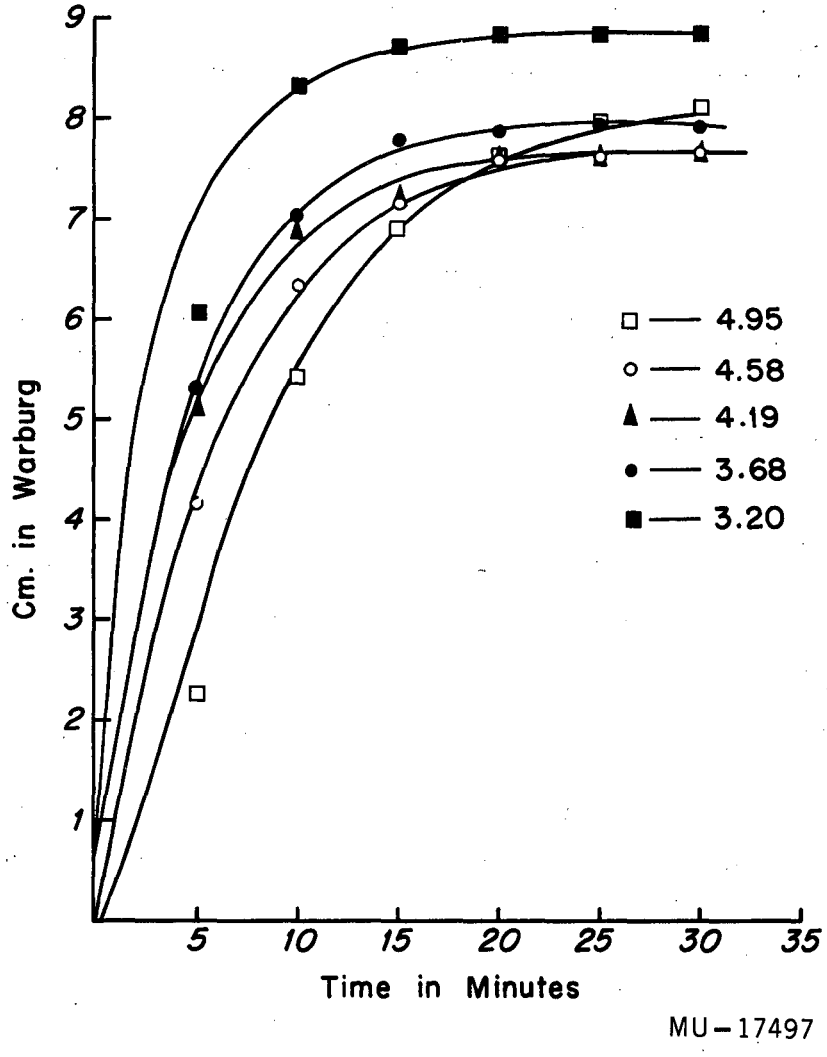

Fig. 24.

The Effect of pH on the Rate of Evolution of CO_2 from CA[GA in Aqueous Citrate Buffers at 0°. k: First-Order Rate Constants 1/sec.

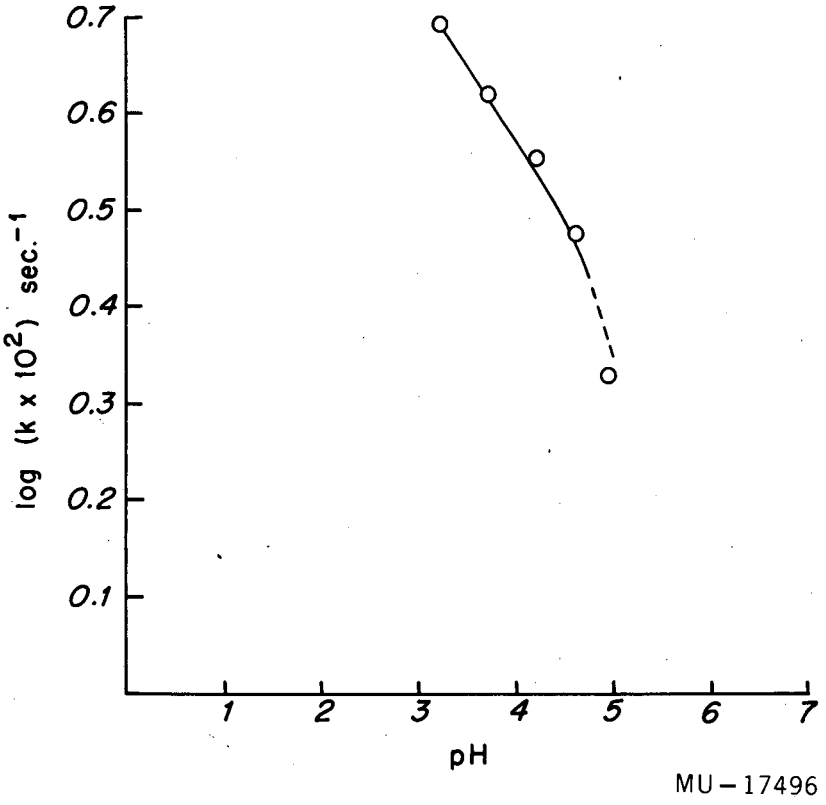

Fig. 25.

reaction upon increase in acidity. The rate constants were calculated by means of the first-order equation

$$k = \frac{2.303}{t} \times \frac{1}{60} \times \text{long} \frac{m_\infty}{m_\infty - m}, \text{ in } 1/\text{sec.}$$

Here, m_∞ is the difference in the readings observed, extrapolated to infinite time; m is the observed difference in readings at time t in minutes.

The effect of the concentration of buffer ions was found to be small so long as the pH was constant. The comparison of the different buffers at the same pH (4.6) showed that the rate decreases in the order: phosphate > citrate $\cong$ acetate.

The rate of decarboxylation of γ-benzyl-N-carboxy-l-glutamate anhydride in citrate buffer was estimated in an attempt to confirm the effect of pH in CALGA. The rates were much slower than those of CALGA and they showed a reverse tendency, i.e., the rate increased with the basicity of the solution in the pH range of 3.20 to 4.95 (Fig. 26).[9]

Discussion

The observed linear relationship of log k vs pH in which k increases with increasing acidity of the solution suggests that the active species in the reaction is the undissociated CALGA. The anion of CALGA may be weak as an electrophilic reagent because of the COO^- group, which masks the electrophylic character of the active carbonyl group.

It might seem curious that the rate is not second-order with respect to CALGA, but if the catalytic effect of water for the reaction is noted, it may be that the water molecule, as a nucleophilic agent, attacks the carbonyl carbon of CALGA in the rate-determining step. Thus, the rate becomes pseudo-first-order in an excess of water:

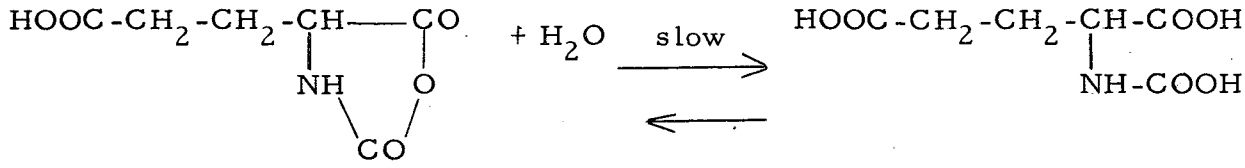

(1)

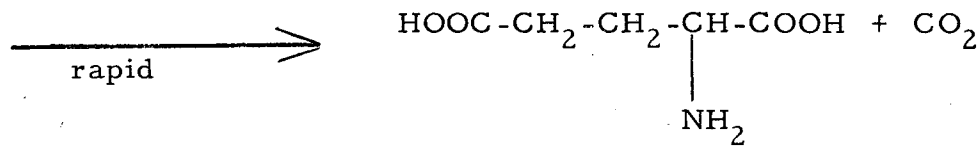

(2)

[9] The reaction of the other N-carboxyamino acid anhydrides with water was found to be subject to general basic catalysis. See P. D. Bartlett and R. H. Jones, J. Am. Chem. Soc. 79, 2153 (1957).

The Effect of pH on the Rate of Evolution of CO_2 from γ-Benzyl /-Glutamate N-Carboxy Anhydride in Aqueous Citrate Buffers at 20°

k: First-Order Rate Constants. $sec.^{-1}$

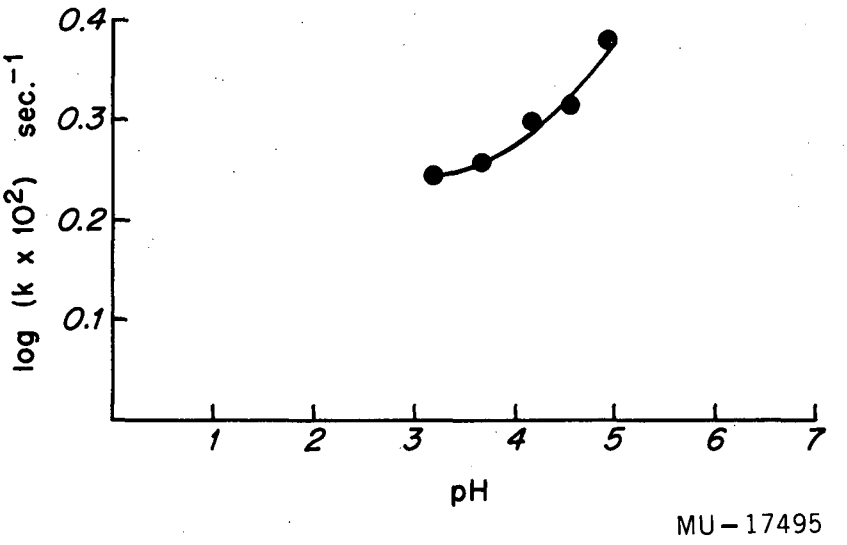

Fig. 26.

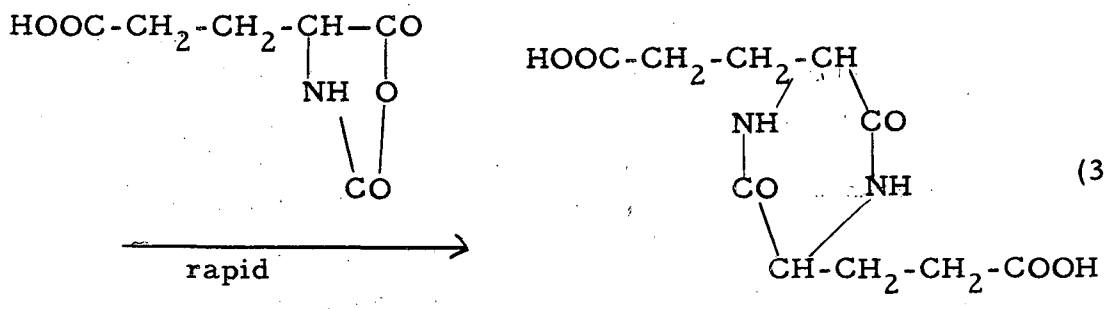

(3)

The amino acid formed in Step (2) acts as a stronger nucleophilic reagent than water, and thus opens the anhydride ring very rapidly and builds up a new ketopiperazine ring. The solubilizing effect of water on the acid may retard the mobility of the CALGA molecule in the solution, thus inhibiting the formation of a macromolecular compound in aqueous solution.

It should be noted, however, that the above consideration is limited to the pH range below 5. The hydroxide ion, which has a stronger nucleophilic tendency than water, may act as the predominant attacking agent in neutral and basic solutions, resulting in a minimum height in the curve for pH vs log k.

This report was prepared as an account of Government sponsored work. Neither the United States, nor the Commission, nor any person acting on behalf of the Commission:

A. Makes any warranty or representation, expressed or implied, with respect to the accuracy, completeness, or usefulness of the information contained in this report, or that the use of any information, apparatus, method, or process disclosed in this report may not infringe privately owned rights; or

B. Assumes any liabilities with respect to the use of, or for damages resulting from the use of any information, apparatus, method, or process disclosed in this report.

As used in the above, "person acting on behalf of the Commission" includes any employee or contractor of the Commission, or employee of such contractor, to the extent that such employee or contractor of the Commission, or employee of such contractor prepares, disseminates, or provides access to, any information pursuant to his employment or contract with the Commission, or his employment with such contractor.